Metal-Insulator Transitions of the Vanadates: New Perspectives of an Old Mystery

Volker Eyert

Center for Electronic Correlations and Magnetism
Institute of Physics, University of Augsburg

November 15, 2010

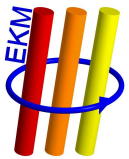

Outline

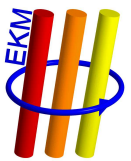

Outline

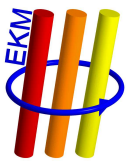

Outline

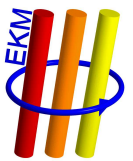

Calculated Electronic Properties

Moruzzi, Janak, Williams (IBM, 1978)

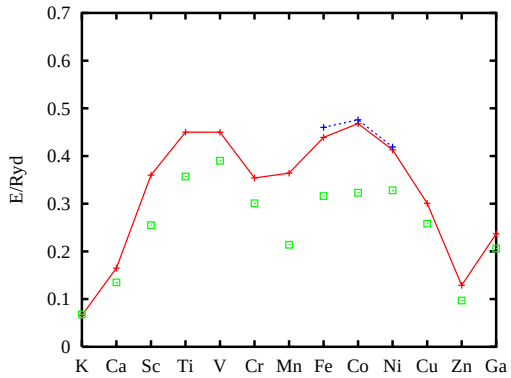

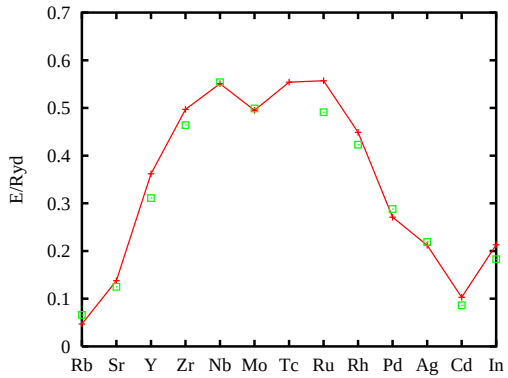

Cohesive Energies
≙ Stability

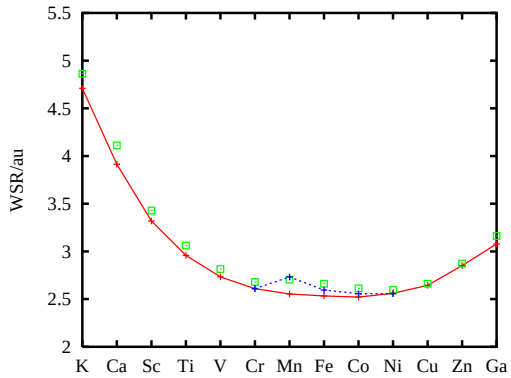

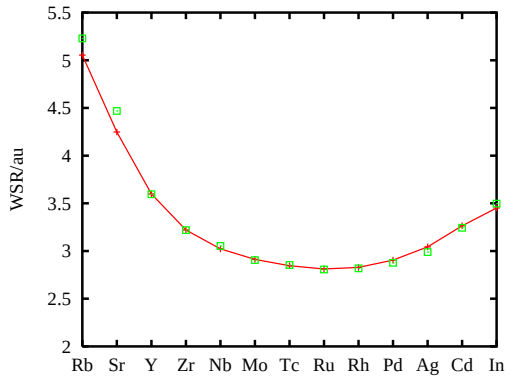

Wigner-Seitz-Rad.
≙ Volume

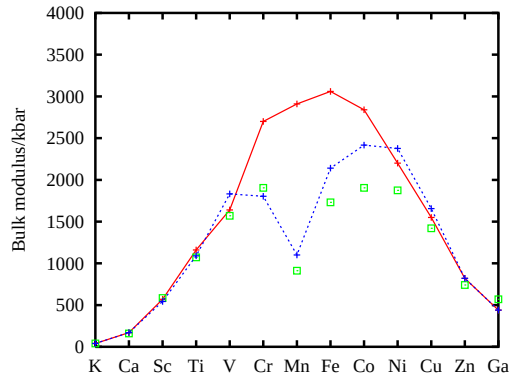

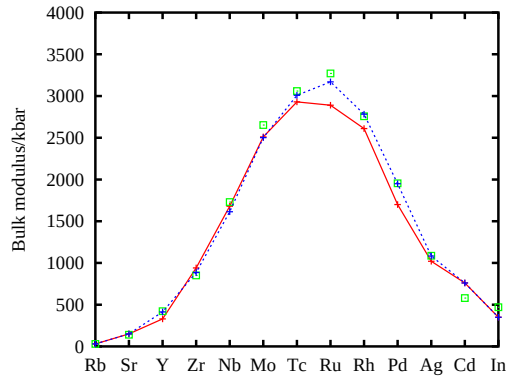

Compressibility
≙ Hardness

Energy band structures from screened HF exchange

Si, AlP, AlAs, GaP, and GaAs

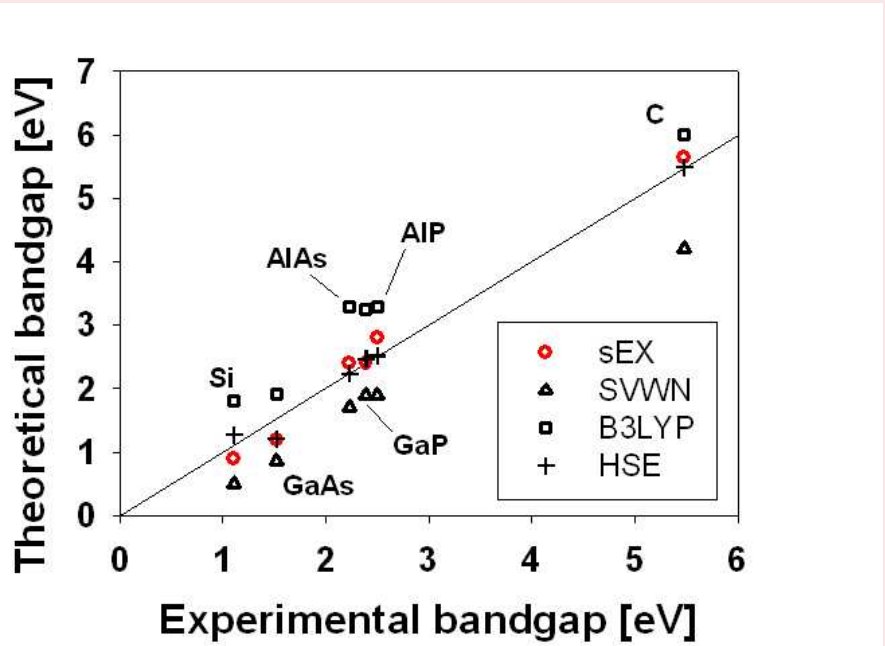

Experimental and theoretical bandgap properties

Shimazaki, Asai
JCP **132**, 224105 (2010)

Key Players

Hamiltonian (within Born-Oppenheimer approximation)

$$\begin{aligned} H &= H_{el,kin} + H_{el-el} + H_{ext} \\ &= \sum_i \left[-\frac{\hbar^2}{2m} \nabla_i^2 \right] + \frac{1}{2} \frac{e^2}{4\pi\epsilon_0} \sum_{\substack{i,j \\ j \neq i}} \frac{1}{|\mathbf{r}_i - \mathbf{r}_j|} + \sum_i v_{ext}(\mathbf{r}_i) \end{aligned}$$

where

$$\sum_i v_{ext}(\mathbf{r}_i) = \frac{1}{2} \frac{e^2}{4\pi\epsilon_0} \sum_{\substack{\mu\nu \\ \mu \neq \nu}} \frac{Z_\mu Z_\nu}{|\mathbf{R}_\mu - \mathbf{R}_\nu|} - \frac{e^2}{4\pi\epsilon_0} \sum_\mu \sum_i \frac{Z_\mu}{|\mathbf{R}_\mu - \mathbf{r}_i|}$$

μ: ions with charge Z_μ, i: electrons

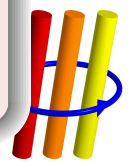

Key Players

Electron Density Operator

$$\hat{\rho}(\mathbf{r}) = \sum_{i=1}^{N} \delta(\mathbf{r} - \mathbf{r}_i) = \sum_{\alpha\beta} \chi^*_\alpha(\mathbf{r}) \chi_\beta(\mathbf{r}) a^+_\alpha a_\beta$$

χ_α: single particle state

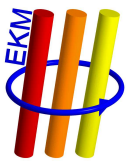

Key Players

Electron Density Operator

$$\hat{\rho}(\mathbf{r}) = \sum_{i=1}^{N} \delta(\mathbf{r} - \mathbf{r}_i) = \sum_{\alpha\beta} \chi^*_\alpha(\mathbf{r}) \chi_\beta(\mathbf{r}) a^+_\alpha a_\beta$$

χ_α: single particle state

Electron Density

$$\rho(\mathbf{r}) = \langle \Psi | \hat{\rho}(\mathbf{r}) | \Psi \rangle = \sum_{\alpha} |\chi_\alpha(\mathbf{r})|^2 n_\alpha$$

$|\Psi\rangle$: many-body wave function, n_α: occupation number

Normalization: $N = \int d^3\mathbf{r}\ \rho(\mathbf{r})$

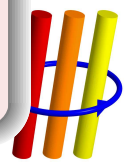

Key Players

Functionals

Universal Functional (independent of ionic positions!)

$$F = \langle \Psi | H_{el,kin} + H_{el-el} | \Psi \rangle$$

Functional due to External Potential:

$$\begin{aligned} \langle \Psi | H_{ext} | \Psi \rangle &= \langle \Psi | \sum_i v_{ext}(\mathbf{r}) \delta(\mathbf{r} - \mathbf{r}_i) | \Psi \rangle \\ &= \int d^3\mathbf{r}\, v_{ext}(\mathbf{r}) \rho(\mathbf{r}) \end{aligned}$$

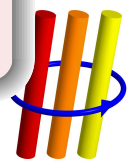

Authors

Pierre C. Hohenberg

Walter Kohn

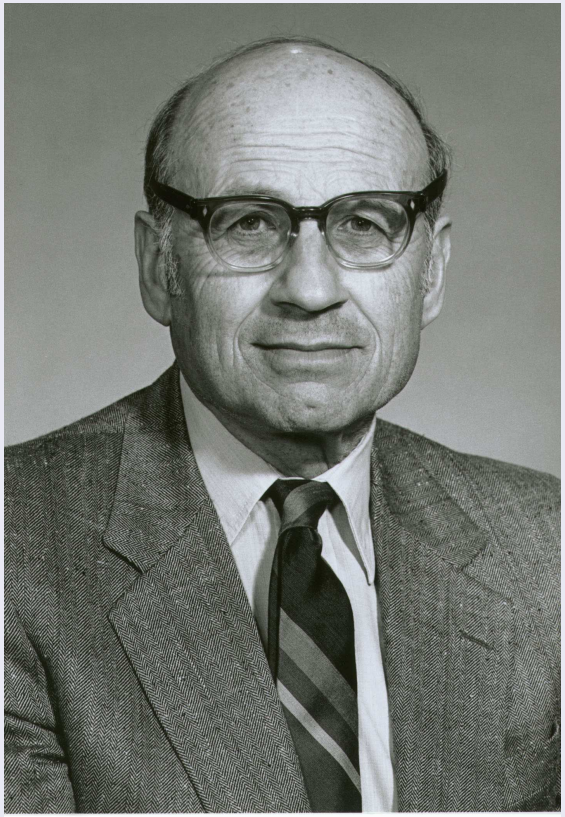

Lu Jeu Sham

Hohenberg and Kohn, 1964: Theorems

1st Theorem

The external potential $v_{ext}(\mathbf{r})$ is determined, apart from a trivial constant, by the electronic ground state density $\rho(\mathbf{r})$.

2nd Theorem

The total energy functional $E[\rho]$ has a minimum equal to the ground state energy at the ground state density.

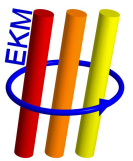

Hohenberg and Kohn, 1964: Theorems

1st Theorem

The external potential $v_{ext}(\mathbf{r})$ is determined, apart from a trivial constant, by the electronic ground state density $\rho(\mathbf{r})$.

2nd Theorem

The total energy functional $E[\rho]$ has a minimum equal to the ground state energy at the ground state density.

Nota bene

Both theorems are formulated for the ground state!

- Zero temperature!
- No excitations!

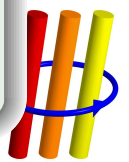

Levy, Lieb, 1979-1983: Constrained Search

Percus-Levy partition

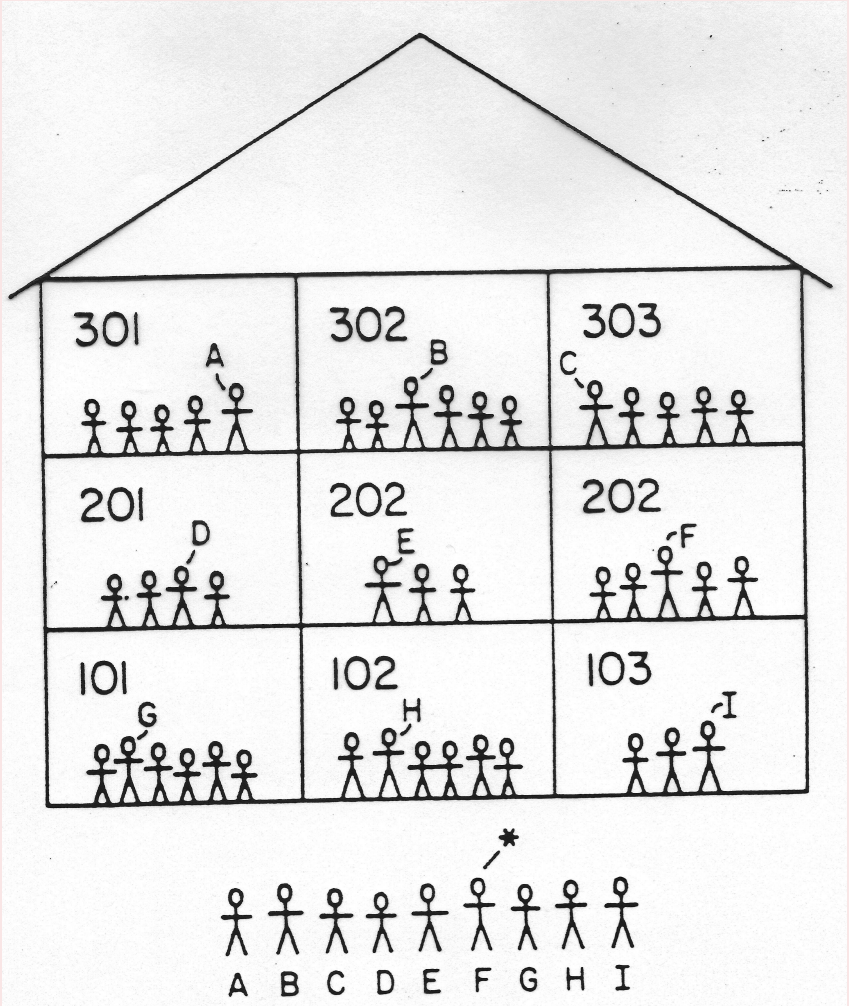

Levy, Lieb, 1979-1983: Constrained Search

Variational principle

$$
\begin{aligned}
E_0 &= \inf_{|\Psi\rangle} \langle\Psi|H|\Psi\rangle \\
&= \inf_{|\Psi\rangle} \langle\Psi|H_{el,kin} + H_{el-el} + H_{ext}|\Psi\rangle \\
&= \inf_{\rho(\mathbf{r})} \left[\inf_{|\Psi\rangle\in S(\rho)} \langle\Psi|H_{el,kin} + H_{el-el}|\Psi\rangle + \int d^3\mathbf{r}\, v_{ext}(\mathbf{r})\rho(\mathbf{r}) \right] \\
&=: \inf_{\rho(\mathbf{r})} \left[F_{LL}[\rho] + \int d^3\mathbf{r}\, v_{ext}(\mathbf{r})\rho(\mathbf{r}) \right] = \inf_{\rho(\mathbf{r})} E[\rho]
\end{aligned}
$$

$S(\rho)$: set of all wave functions leading to density ρ
$F_{LL}[\rho]$: Levy-Lieb functional

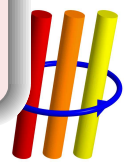

Levy, Lieb, 1979-1983: Constrained Search

Levy-Lieb functional

$$
\begin{aligned}
F_{LL}[\rho] &= \inf_{|\Psi\rangle \in S(\rho)} \langle \Psi | H_{el,kin} + H_{el-el} | \Psi \rangle \\
&= \underbrace{T[\rho] + W_{xc}[\rho]} + \frac{1}{2} \frac{e^2}{4\pi\epsilon_0} \int d^3\mathbf{r} \int d^3\mathbf{r}' \, \frac{\rho(\mathbf{r})\rho(\mathbf{r}')}{|\mathbf{r}-\mathbf{r}'|} \\
&= G[\rho] + \frac{1}{2} \frac{e^2}{4\pi\epsilon_0} \int d^3\mathbf{r} \int d^3\mathbf{r}' \, \frac{\rho(\mathbf{r})\rho(\mathbf{r}')}{|\mathbf{r}-\mathbf{r}'|}
\end{aligned}
$$

Functionals

- Kinetic energy funct.: $T[\rho]$ — not known!
- Exchange-correlation energy funct.: $W_{xc}[\rho]$ — not known!
- Hartree energy funct.: $\frac{1}{2} \frac{e^2}{4\pi\epsilon_0} \int d^3\mathbf{r} \int d^3\mathbf{r}' \, \frac{\rho(\mathbf{r})\rho(\mathbf{r}')}{|\mathbf{r}-\mathbf{r}'|}$ — known!

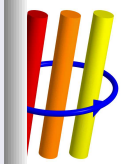

Kohn and Sham, 1965: Single-Particle Equations

Ansatz

1. use different splitting of the functional $G[\rho]$

$$T[\rho] + W_{xc}[\rho] = G[\rho] \stackrel{!}{=} T_0[\rho] + E_{xc}[\rho]$$

2. reintroduce single-particle wave functions

Imagine: non-interacting electrons with same density

- Density: $\rho(\mathbf{r}) = \sum_\alpha^{occ} |\chi_\alpha(\mathbf{r})|^2$ known!
- Kinetic energy funct.:
  $T_0[\rho] = \sum_\alpha^{occ} \int d^3\mathbf{r}\, \chi_\alpha^*(\mathbf{r}) \left[-\frac{\hbar^2}{2m}\nabla^2\right] \chi_\alpha(\mathbf{r})$ known!
- Exchange-correlation energy funct.: $E_{xc}[\rho]$ not known!

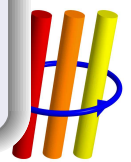

Kohn and Sham, 1965: Single-Particle Equations

Euler-Lagrange Equations (Kohn-Sham Equations)

$$\frac{\delta E[\rho]}{\delta \chi_\alpha^*(\mathbf{r})} - \varepsilon_\alpha \chi_\alpha(\mathbf{r}) = \left[-\frac{\hbar^2}{2m}\nabla^2 + v_{eff}(\mathbf{r}) - \varepsilon_\alpha \right] \chi_\alpha(\mathbf{r}) \stackrel{!}{=} 0$$

- Effective potential: $v_{eff}(\mathbf{r}) := v_{ext}(\mathbf{r}) + v_H(\mathbf{r}) + v_{xc}(\mathbf{r})$
- Exchange-correlation potential: not known!

$$v_{xc}(\mathbf{r}) := \frac{\delta E_{xc}[\rho]}{\delta \rho}$$

- „Single-particle energies“:
  ε_α (Lagrange-parameters, orthonormalization)

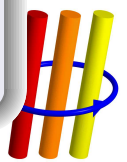

Kohn and Sham, 1965: Local Density Approximation

Be Specific!

- Approximate exchange-correlation energy functional

$$E_{xc}[\rho] = \int \rho(\mathbf{r}) \varepsilon_{xc}(\rho(\mathbf{r})) d^3\mathbf{r}$$

- Exchange-correlation energy density $\varepsilon_{xc}(\rho(\mathbf{r}))$
  - depends on local density only!
  - is calculated from homogeneous, interacting electron gas
- Exchange-correlation potential

$$v_{xc}(\rho(\mathbf{r})) = \left[\frac{\partial}{\partial \rho} \{\rho \varepsilon_{xc}(\rho)\} \right]_{\rho=\rho(\mathbf{r})}$$

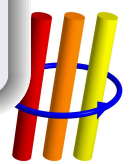

Kohn and Sham, 1965: Local Density Approximation

Limitations and Beyond

- LDA exact for homogeneous electron gas (within QMC)
- Spatial variation of ρ ignored
  - $\rightarrow$ include $\nabla\rho(\mathbf{r}), \ldots$
  - $\rightarrow$ Generalized Gradient Approximation (GGA)
- Self-interaction cancellation in $v_{Hartree} + v_x$ violated

Si

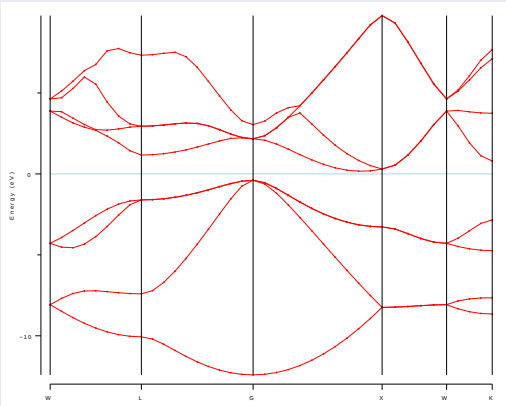

Bandgaps

- Si, exp: 1.11 eV
- Si, GGA: 0.57 eV
- Ge, exp: 0.67 eV
- Ge, GGA: 0.09 eV

Ge

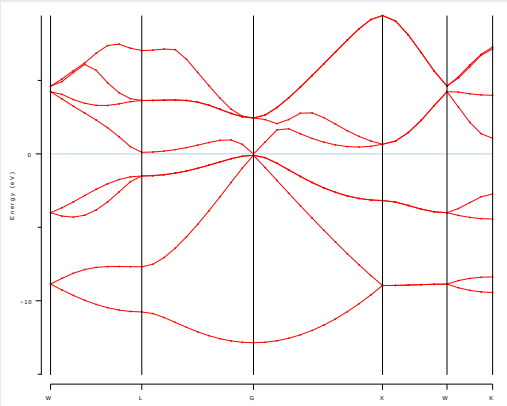

Muffin-Tin Approximation

John C. Slater

Full Potential

$$v_\sigma(\mathbf{r}) : \begin{cases} \text{spherical symmetric near nuclei} \\ \text{flat outside the atomic cores} \end{cases}$$

Muffin-Tin Approximation

$$v_\sigma^{MT}(\mathbf{r}) = \begin{cases} \text{spherical symmetric in spheres} \\ \text{constant in interstitial region} \end{cases}$$

Muffin-Tin Approximation

Full Potential (FeS_2)

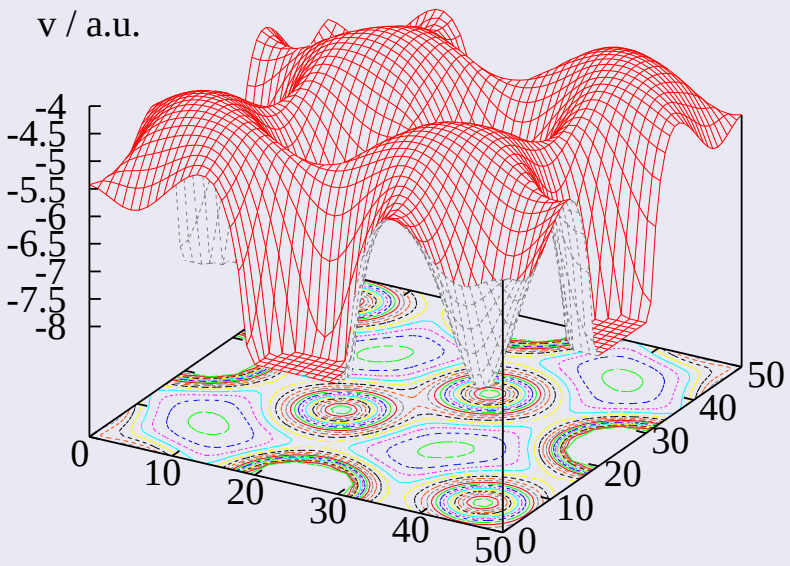

Muffin-Tin Potential

Muffin-Tin Approximation

Wave Function

1. solve Schrödingers eq.
   → partial waves
2. match partial waves
   → basis functions,
   „augmented“ partial waves
3. use to expand
   → wave function

Muffin-Tin Potential

Muffin-Tin Approximation

Flavors

- Muffin-Tin Approximation: touching spheres
- Atomic Sphere Approximation: space-filling spheres
  - interstitial region formally removed
  - only numerical functions in spheres
  - minimal basis set (s, p, d)
    - very high computational efficiency $\rightarrow \mathcal{O}$(ASA) speed!!!
  - makes potential more realistic
  - systematic error in total energy bad!

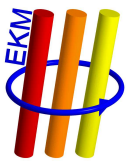

Iron Pyrite: FeS_2

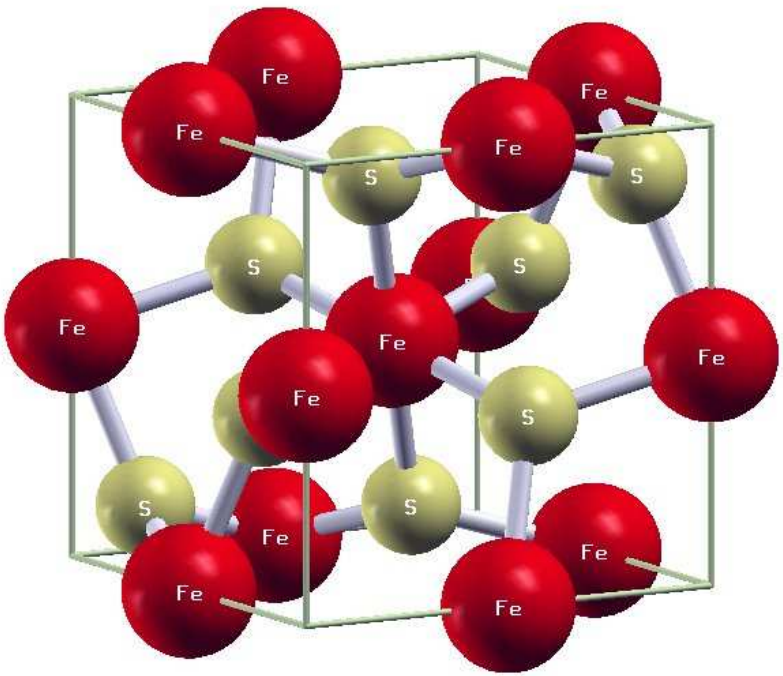

Pyrite

- $Pa\bar{3}$ (T_h^6)
- a = 5.4160 Å
- "NaCl structure" sublattices occupied by
  - iron atoms
  - sulfur pairs
- sulfur pairs $\parallel \langle 111 \rangle$ axes
- x_S = 0.38484
- rotated FeS_6 octahedra

FeS_2: Structure Optimization

ASA^+ Code

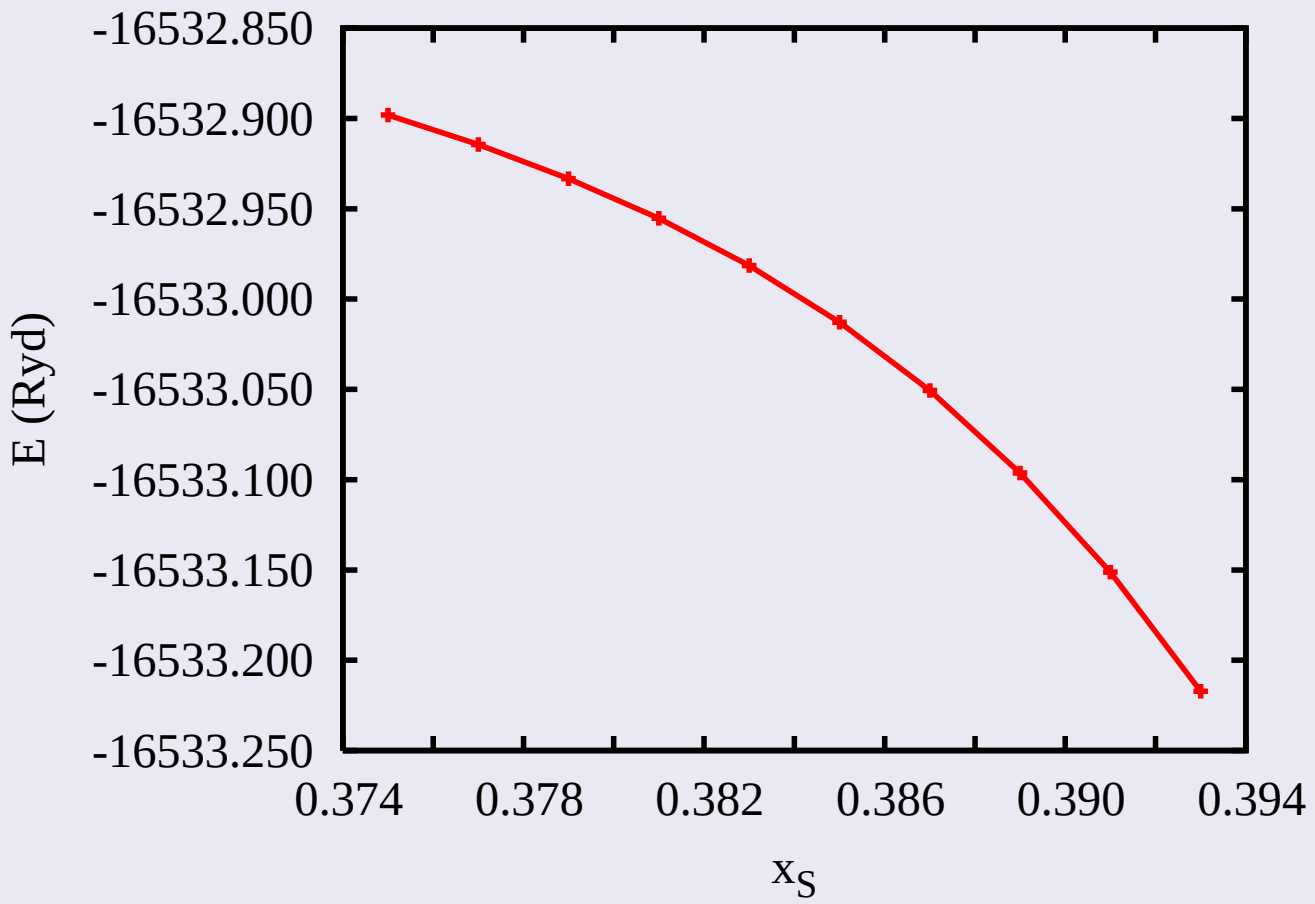

Basic Principles of the Full-Potential ASW Method

Steps to be Taken

- remove total energy error due to overlap of atomic spheres
  - reintroduce non-overlapping muffin-tin spheres
  - restore interstitial region

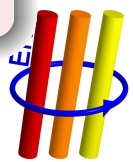

Basic Principles of the Full-Potential ASW Method

Steps to be Taken

- remove total energy error due to overlap of atomic spheres
  - reintroduce non-overlapping muffin-tin spheres
  - restore interstitial region
- find representation of electron density and full potential
  - inside muffin-tin spheres
  - in the interstitial region

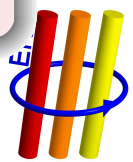

Basic Principles of the Full-Potential ASW Method

Steps to be Taken

- remove total energy error due to overlap of atomic spheres
  - reintroduce non-overlapping muffin-tin spheres
  - restore interstitial region
- find representation of electron density and full potential
- find representation of products of the wave function
  - inside muffin-tin spheres
  - in the interstitial region

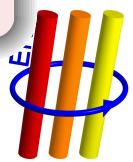

Basic Principles of the Full-Potential ASW Method

Steps to be Taken

- remove total energy error due to overlap of atomic spheres
  - reintroduce non-overlapping muffin-tin spheres
  - restore interstitial region
- find representation of electron density and full potential
- find representation of products of the wave function
- find representation of products of the basis functions
  - inside muffin-tin spheres
  - in the interstitial region

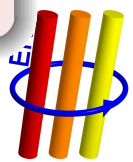

Basic Principles of the Full-Potential ASW Method

Steps to be Taken

- remove total energy error due to overlap of atomic spheres
  - reintroduce non-overlapping muffin-tin spheres
  - restore interstitial region
- find representation of electron density and full potential
- find representation of products of the wave function
- find representation of products of the basis functions
  - inside muffin-tin spheres
    - use spherical-harmonics expansions
  - in the interstitial region

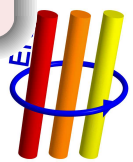

Basic Principles of the Full-Potential ASW Method

Steps to be Taken

- remove total energy error due to overlap of atomic spheres
  - reintroduce non-overlapping muffin-tin spheres
  - restore interstitial region
- find representation of electron density and full potential
- find representation of products of the wave function
- find representation of products of the basis functions
  - inside muffin-tin spheres
    - use spherical-harmonics expansions
  - in the interstitial region
    - no exact spherical-wave representation available!

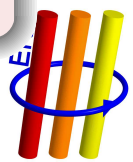

From Wave Functions to Electron Density

Density inside MT-Spheres (Al)

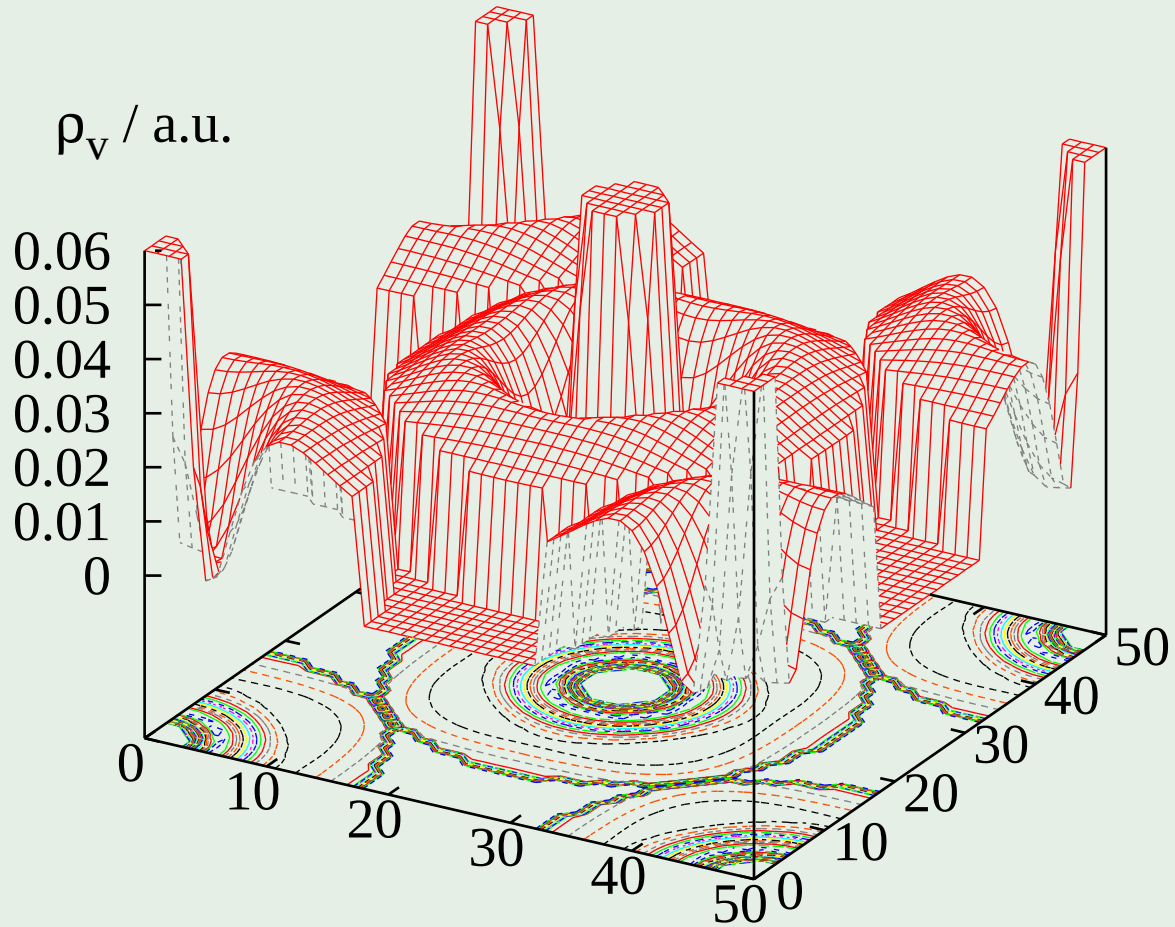

From Wave Functions to Electron Density

Products of Spherical Waves in Interstitial Region

- expand in spherical waves
  - would be efficient
  - coefficients/integrals not known analytically
  - Methfessel, 1988:
    match values and slopes at MT-sphere surfaces

From Wave Functions to Electron Density

Products of Spherical Waves in Interstitial Region

- expand in spherical waves
  - match values and slopes at MT-sphere surfaces

Density from Value/Slope Matching at MT-Radii (Al)

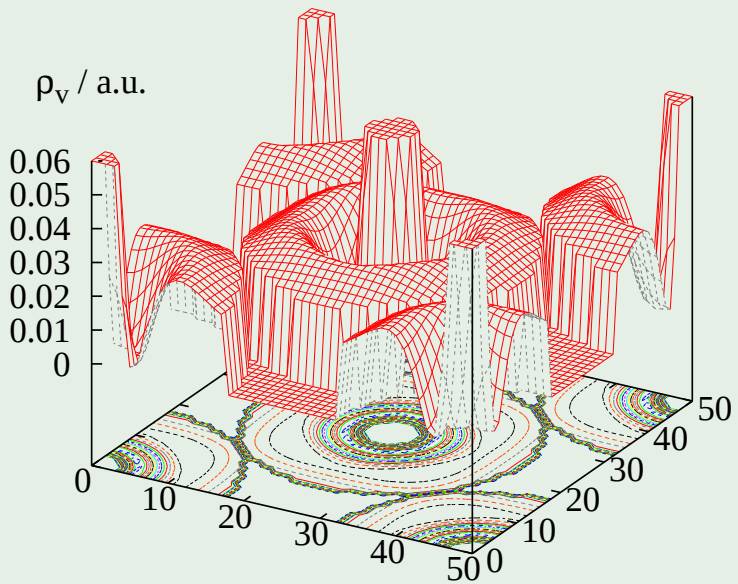

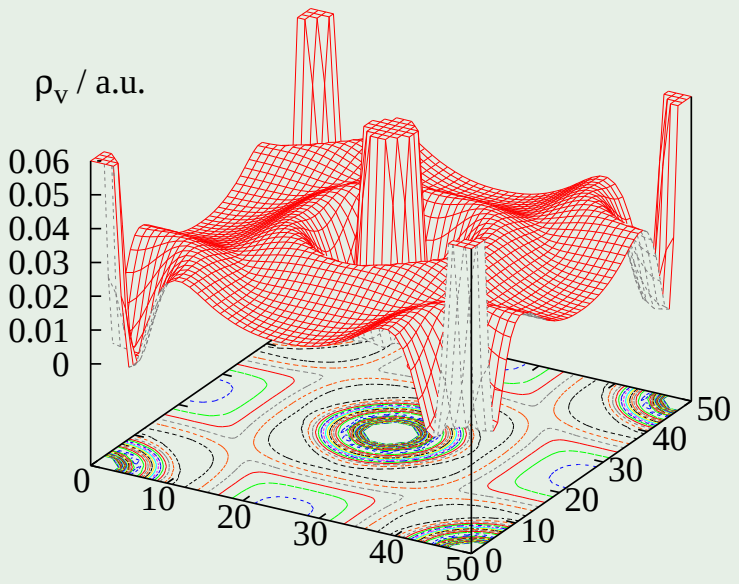

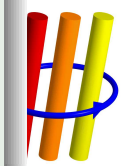

Comparison of Approaches

Ole K. Andersen 1975

- ASA geometry used for basis functions
  → minimal basis set good!
- ASA geometry used for density and potential
  → error in total energy bad!

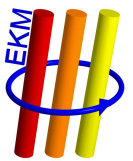

Comparison of Approaches

Ole K. Andersen 1975

- ASA geometry used for basis functions
  → minimal basis set good!
- ASA geometry used for density and potential
  → error in total energy bad!

Michael S. Methfessel 1988

- MT geometry used for density and potential
  → accurate total energy good!
- MT geometry used for basis functions
  → large basis set bad!

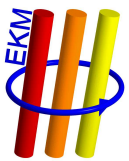

Comparison of Approaches

Ole K. Andersen — 1975

- ASA geometry used for basis functions — good!
- ASA geometry used for density and potential — bad!

Michael S. Methfessel — 1988

- MT geometry used for density and potential — good!
- MT geometry used for basis functions — bad!

present approach — 2006

- ASA geometry used for basis functions
  $\rightarrow$ minimal basis set $\rightarrow$ $\mathcal{O}$(ASA) speed — great!
- MT geometry used for density and potential
  $\rightarrow$ accurate total energy — great!

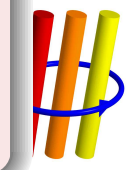

Implementation: Augmented Spherical Wave Method

0th Generation ASW (Williams, Kübler, Gelatt, 1970s)

PRB **19**, 6094 (1979)

1st Generation (VE, 1990s)

- new implementation (accurate, stable, portable)
  VE, Int. J. Quantum Chem. **77**, 1007 (2000)
  VE, Lect. Notes Phys. **719** (Springer, 2007)
- xAnderson convergence acceleration scheme
  VE, J. Comput. Phys. **124**, 271 (1996)
- all LDA- and GGA-parametrizations
- still based on atomic-sphere approximation
  VE, Höck, PRB **57**, 12727 (1998)

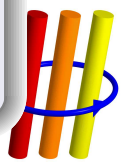

Implementation: Augmented Spherical Wave Method

2nd Generation ASW (VE, 2000s)

- based on 1st generation code
- full-potential ASW method — at $\mathcal{O}$(ASA) speed!
  - electron densities, spin densities
  - electric field gradients
  - elastic properties, phonon spectra
- optical properties
  - based on linear-response theory
  - direct calculation of $\Re\sigma$ and $\Im\sigma$
  - no Kramers-Kronig relations needed
- transport properties, thermoelectrics
- LDA+U method
  - all „flavors“ for double-counting terms (AMF, FLL, DFT)

VE, Lect. Notes Phys. (2nd ed., Springer, 2011)

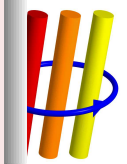

ASW Method: Further Reading

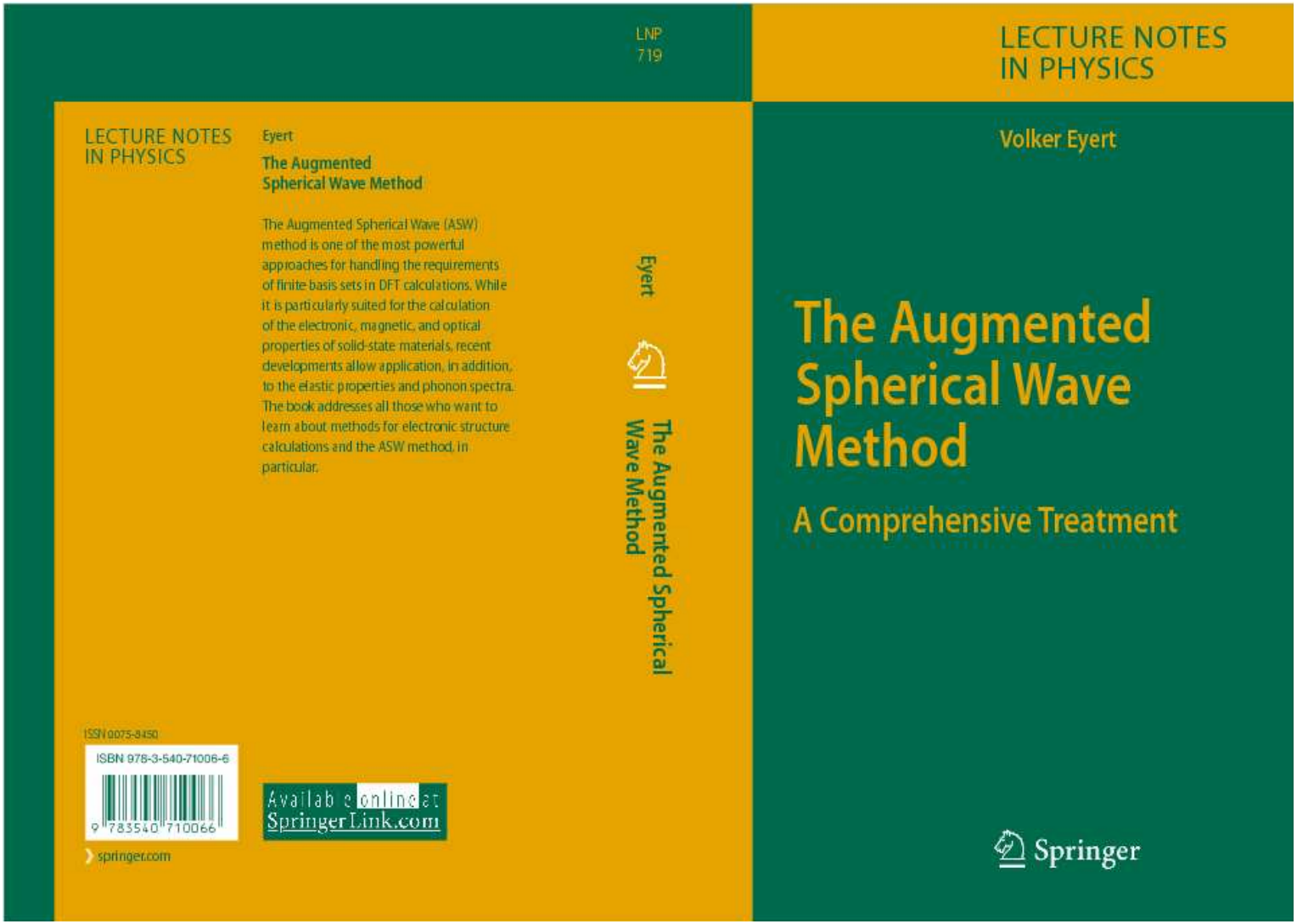

Iron Pyrite: FeS_2

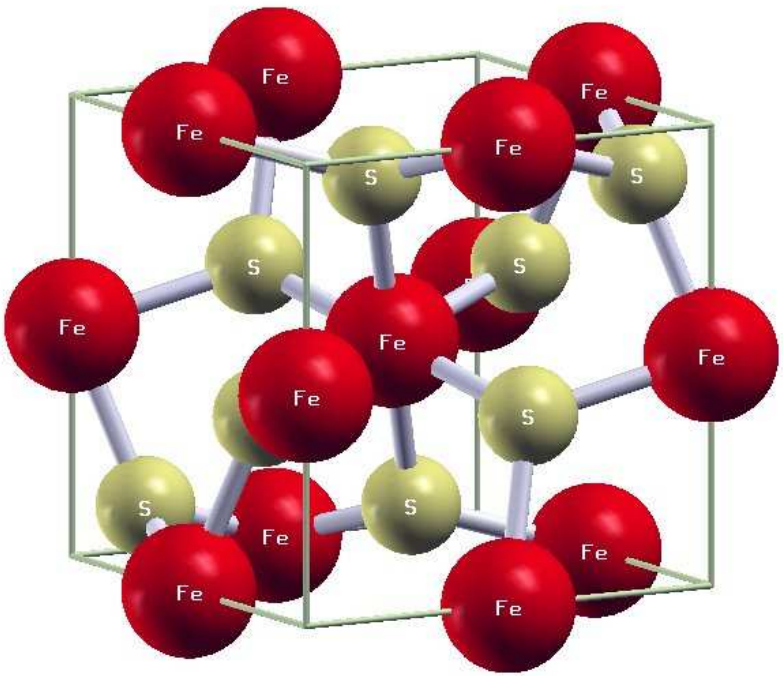

Pyrite

- $Pa\bar{3}$ (T_h^6)
- a = 5.4160 Å
- "NaCl structure" sublattices occupied by
  - iron atoms
  - sulfur pairs
- sulfur pairs $\parallel \langle 111 \rangle$ axes
- x_S = 0.38484
- rotated FeS_6 octahedra

FeS_2: Structure Optimization

ASA^+ Code

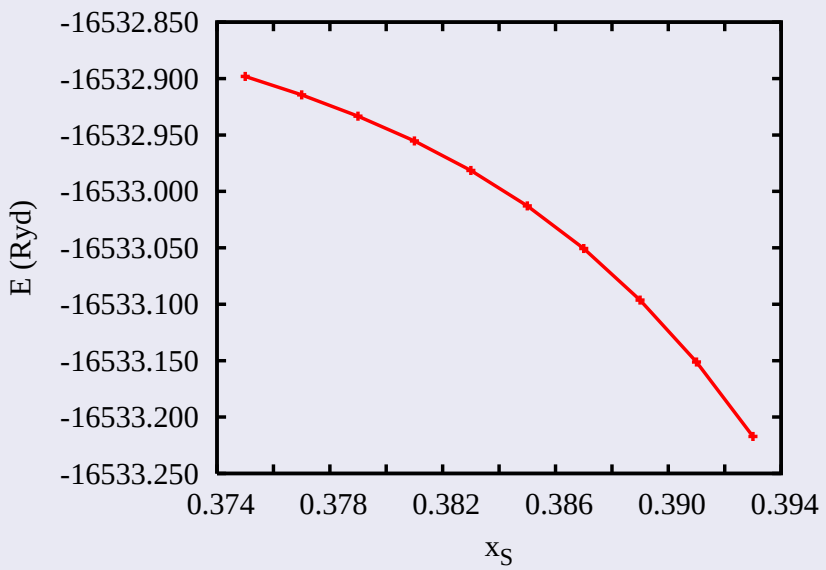

FeS_2: Structure Optimization

ASA$^+$ Code

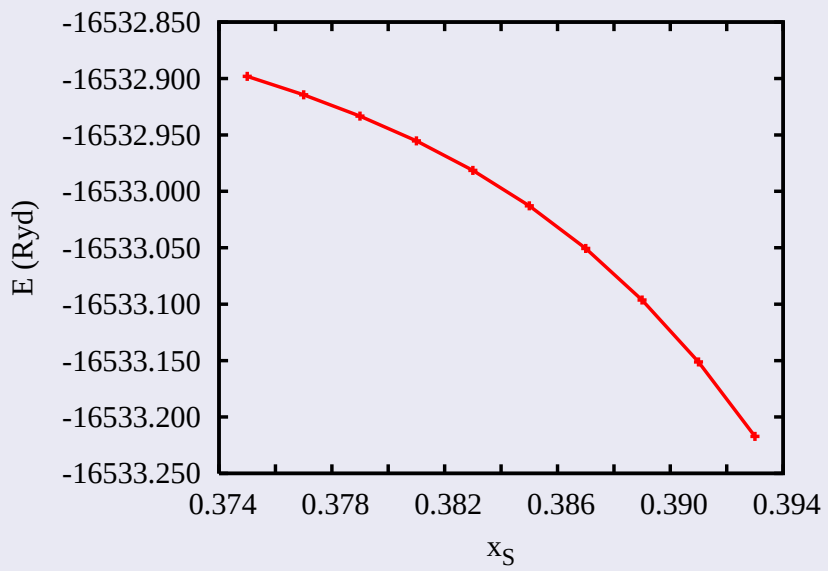

Full-Potential Code

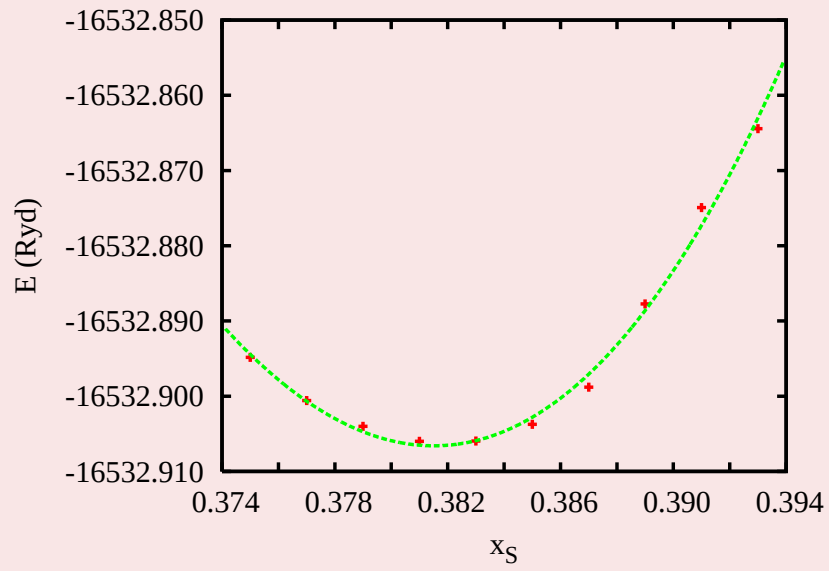

at $\mathcal{O}$(ASA) speed!

Phase Stability in Silicon

ASA$^+$ Code

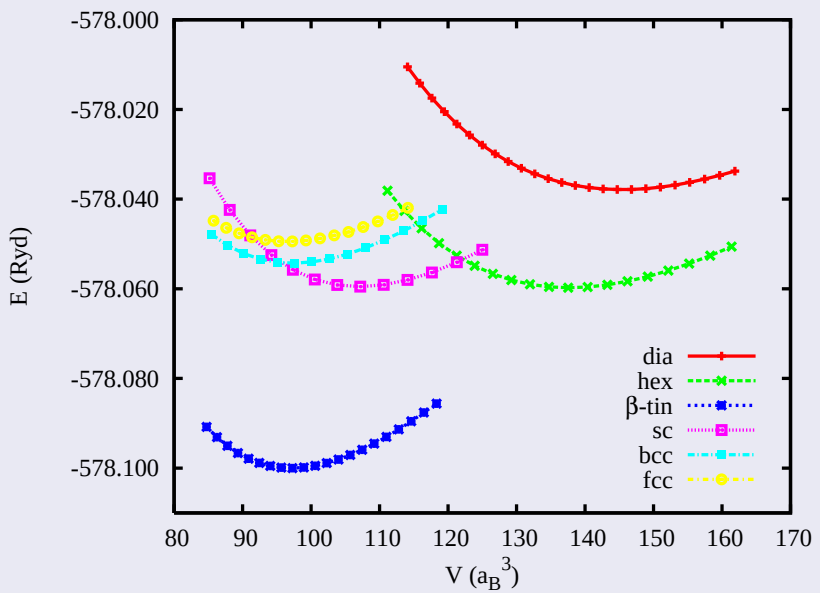

Bad

- β-tin structure most stable # nature (diamond structure)

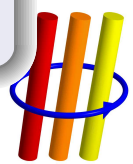

Phase Stability in Silicon

ASA$^+$ Code

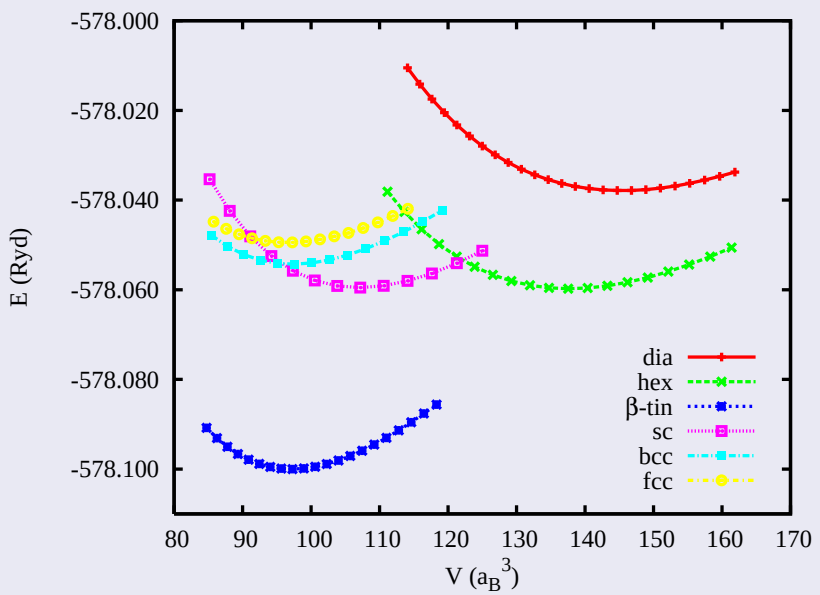

Full-Potential Code

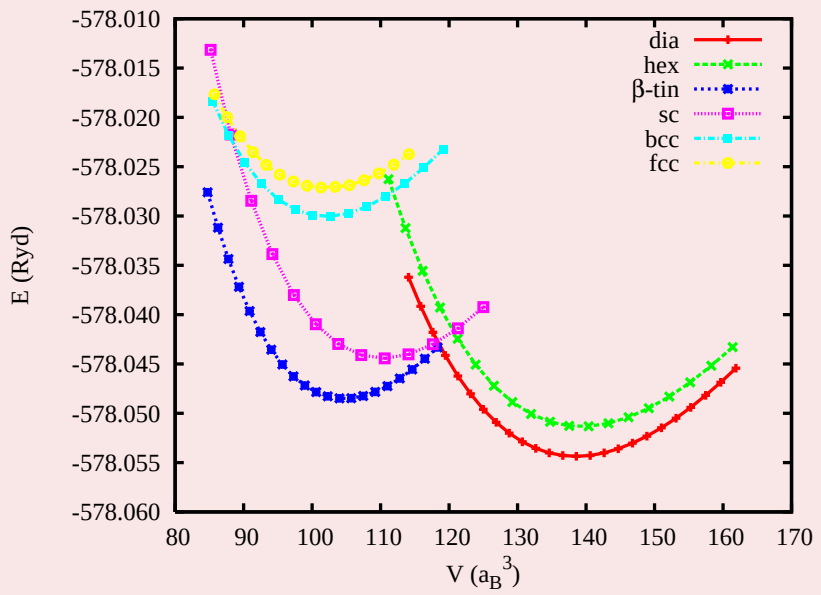

New! at $\mathcal{O}$(ASA) speed!

- diamond structure most stable
- pressure induced phase transition to β-tin structure

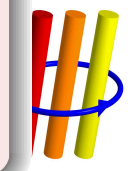

LTO(Γ)-Phonon in Silicon

ASA$^+$ Code

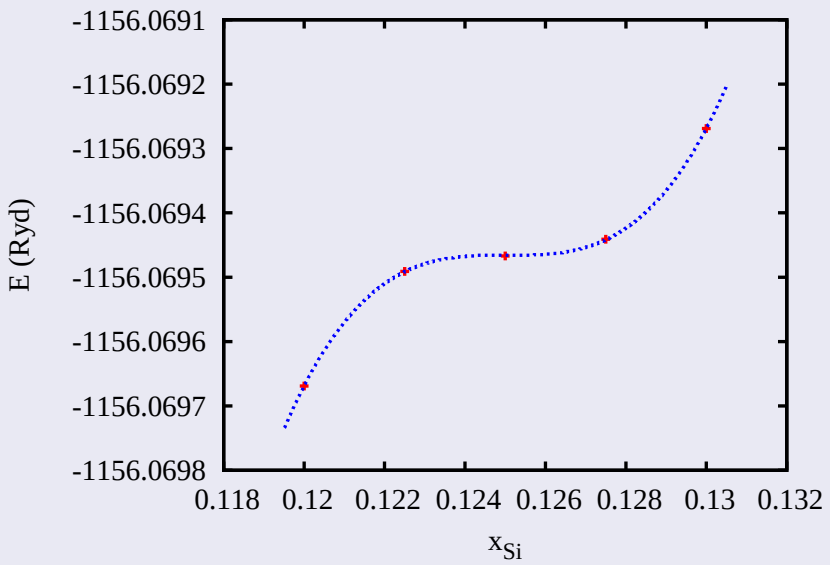

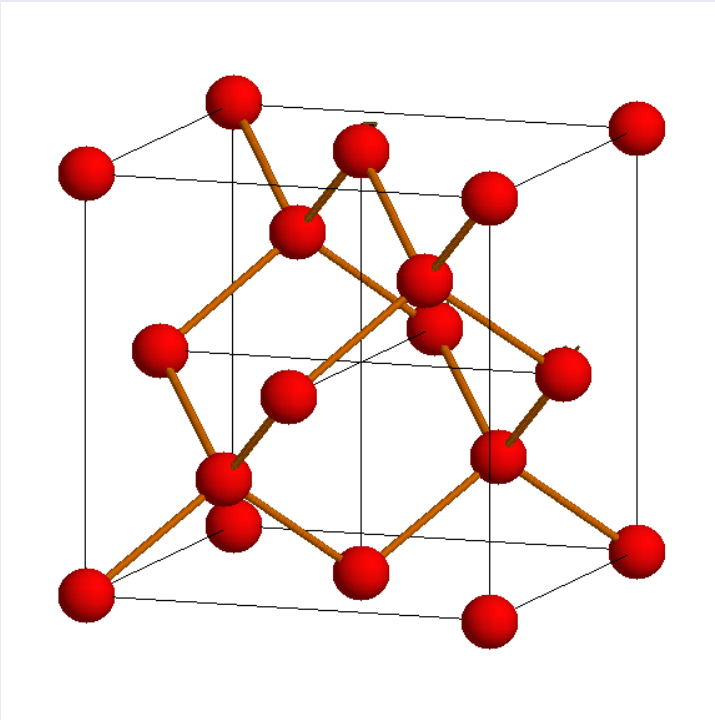

Bad

- no stable Si position # nature

LTO(Γ)-Phonon in Silicon

ASA$^+$ Code

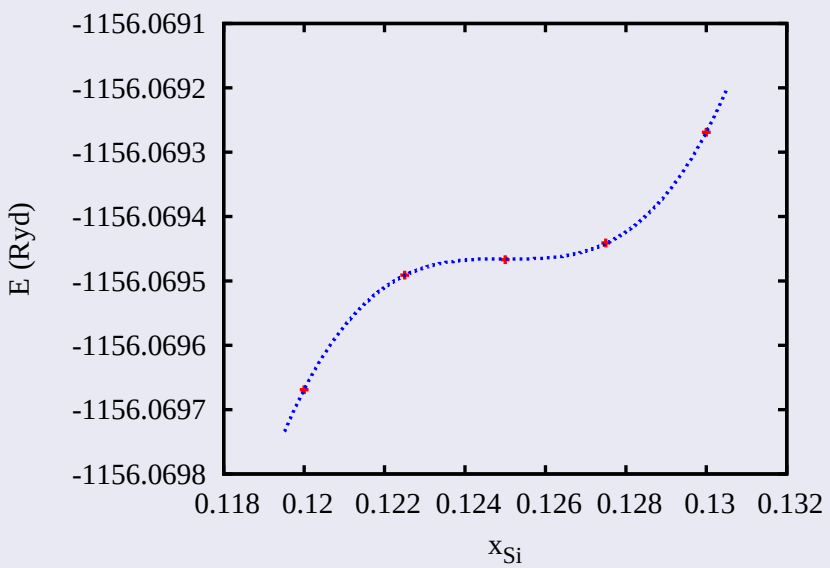

Full-Potential Code

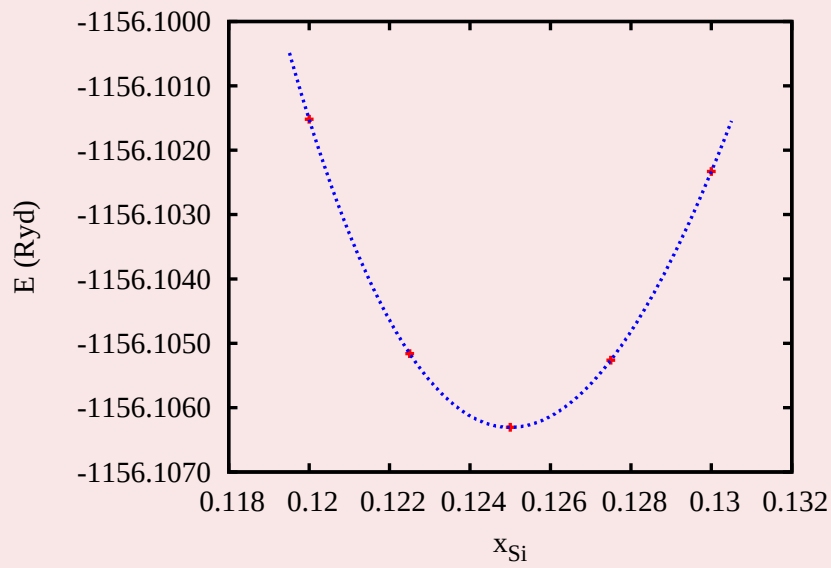

New! at $\mathcal{O}$(ASA) speed!

- phonon frequency: $f_{calc} = 15.34\,\text{THz}$ ($f_{exp} = 15.53\,\text{THz}$)

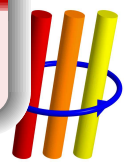

Outline

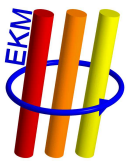

Metal-Insulator Transition of VO_2

Morin, PRL 1959

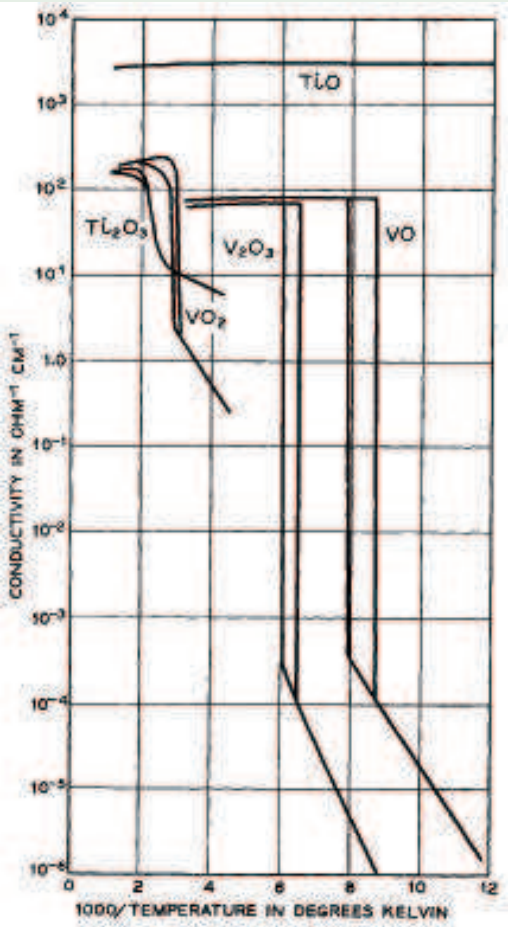

Metal-Insulator Transitions (MIT)

- VO_2 (d^1)
  - 1st order, 340 K, $\Delta\sigma \approx 10^4$
  - rutile $\longrightarrow$ M_1 (monoclinic)
- V_2O_3 (d^2)
  - 1st order, 170 K, $\Delta\sigma \approx 10^6$
  - corundum $\longrightarrow$ monoclinic
  - paramagn. $\longrightarrow$ AF order

Origin of the MIT???

- Structural Changes?
- Electron Correlations?

Metal-Insulator Transition of VO_2

Octahedral Coordination

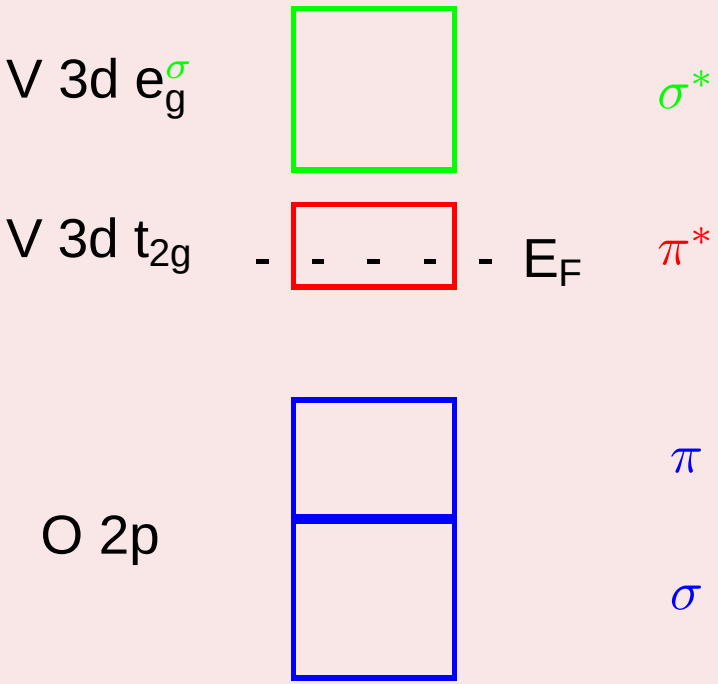

- V 3*d*-O 2*p* hybridization
  - σ, σ^* (p-de_g^σ)
  - π, π^* (p-dt_{2g})

Rutile Structure

- simple tetragonal
- $P4_2/mnm$ (D_{4h}^{14})

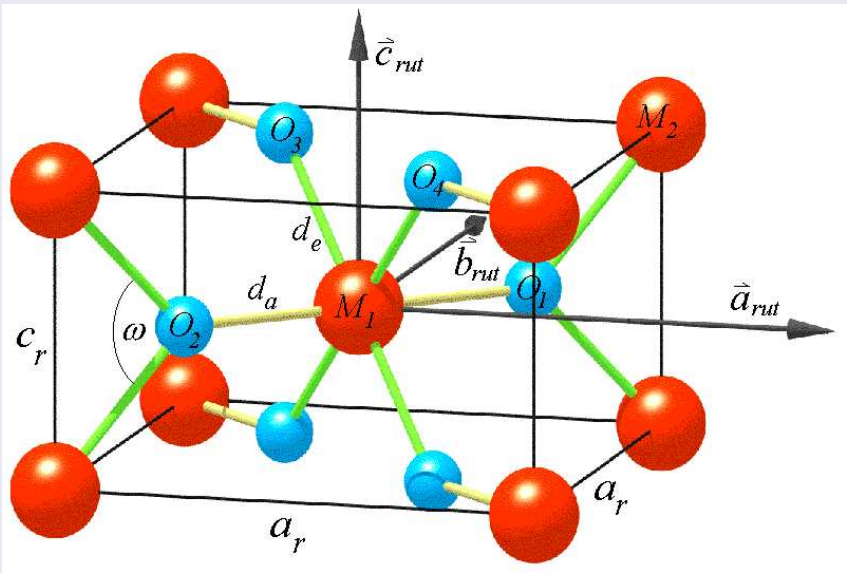

Metal-Insulator Transition of VO_2

Octahedral Coordination

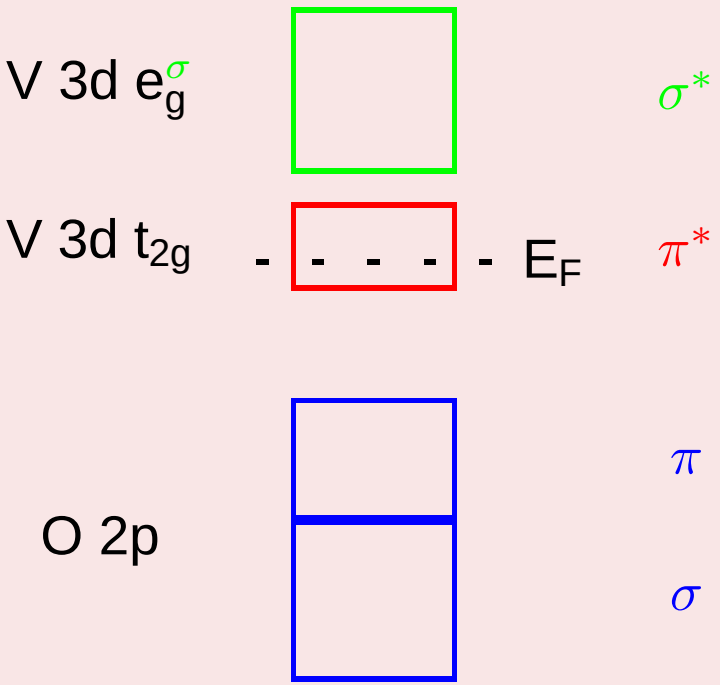

- V 3*d*-O 2*p* hybridization
  - σ, σ^* (p-de_g^σ)
  - π, π^* (p-dt_{2g})

e_g^σ Orbitals

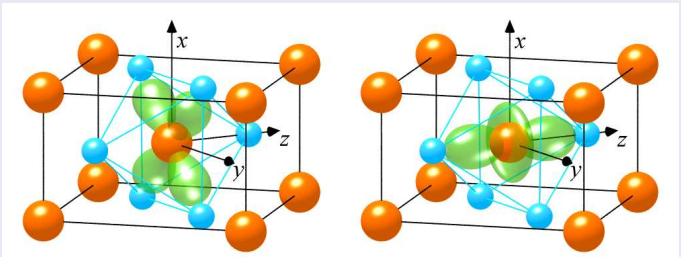

t_{2g} Orbitals

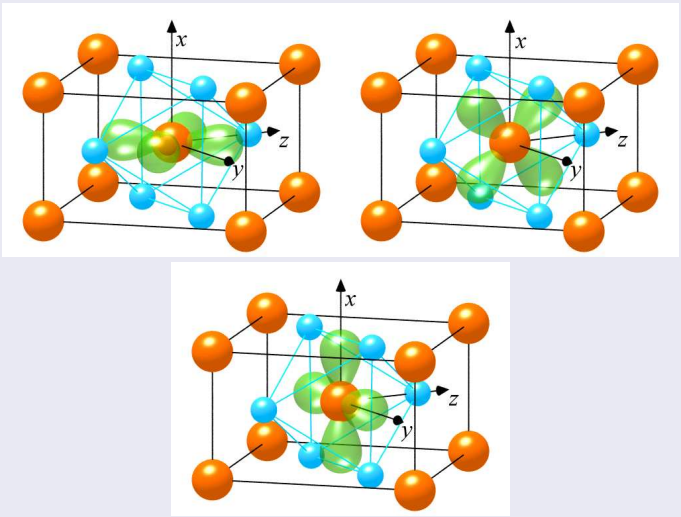

Metal-Insulator Transition of VO_2

Octahedral Chains

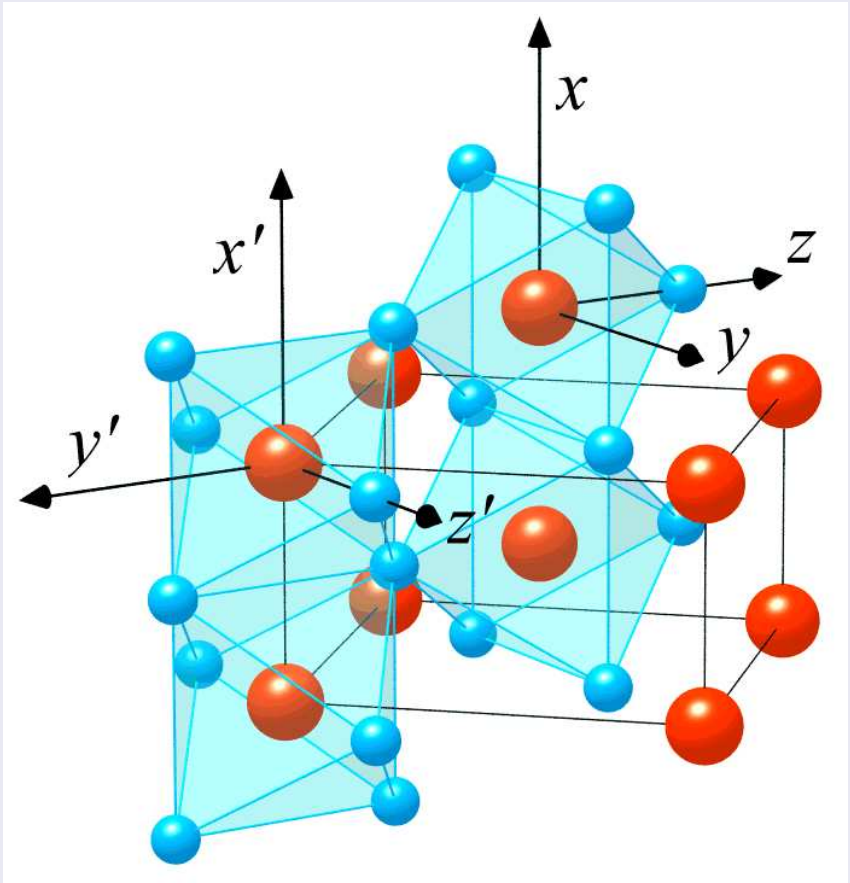

Rutile Structure

- simple tetragonal
- $P4_2/mnm$ (D_{4h}^{14})

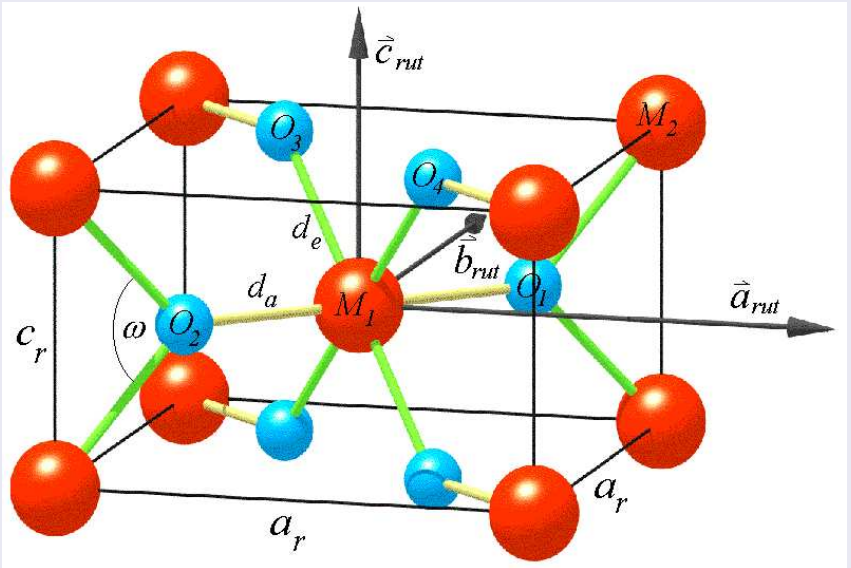

Metal-Insulator Transition of VO_2

Octahedral Coordination

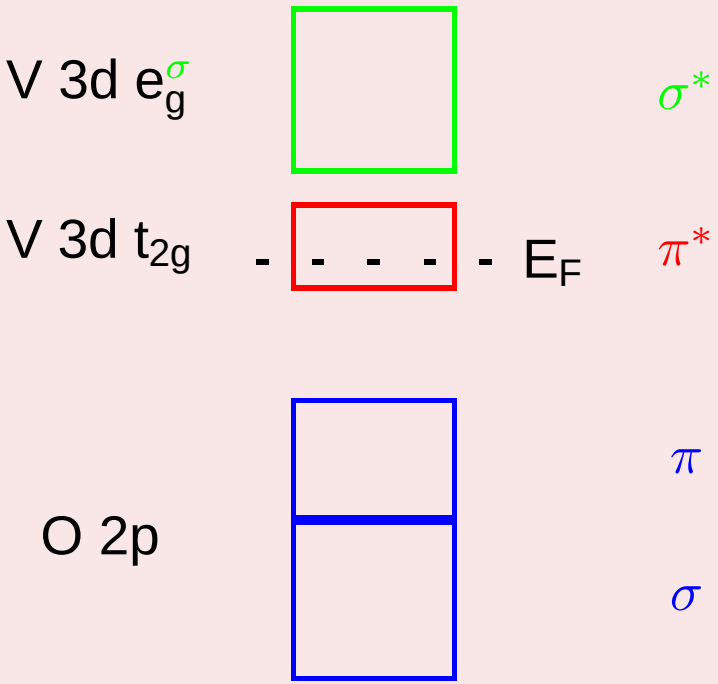

t_{2g} Orbitals

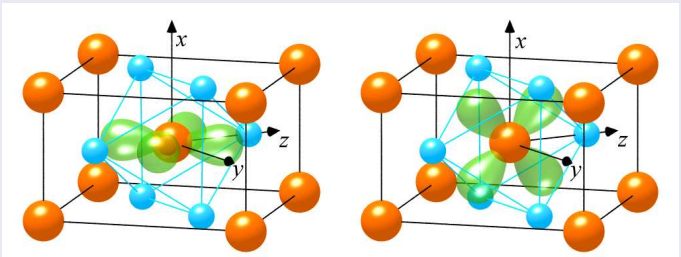

$e_g^\pi = \text{“}\pi^*\text{”}$

$a_{1g} = \text{“}d_\parallel\text{”}$

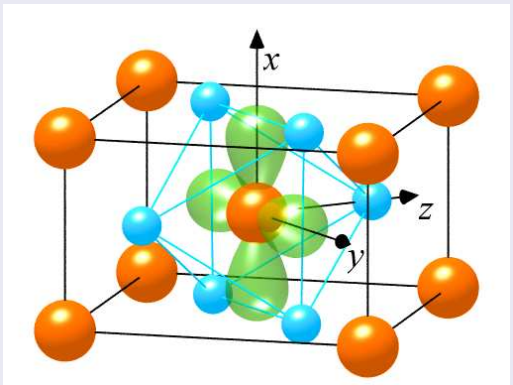

Metal-Insulator Transition of VO_2

Rutile Structure

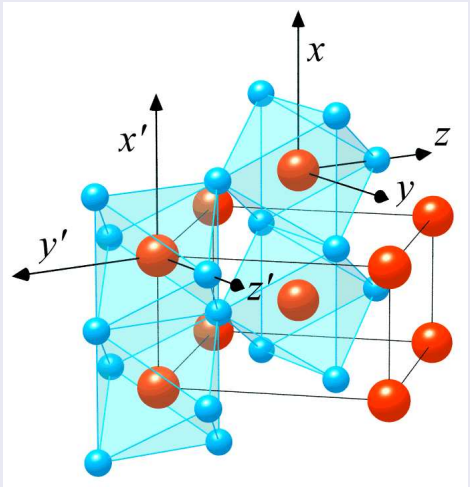

Structural Changes

- V-V dimerization $\parallel c_R$
- antiferroelectric displacement $\perp c_R$

M_1-Structure

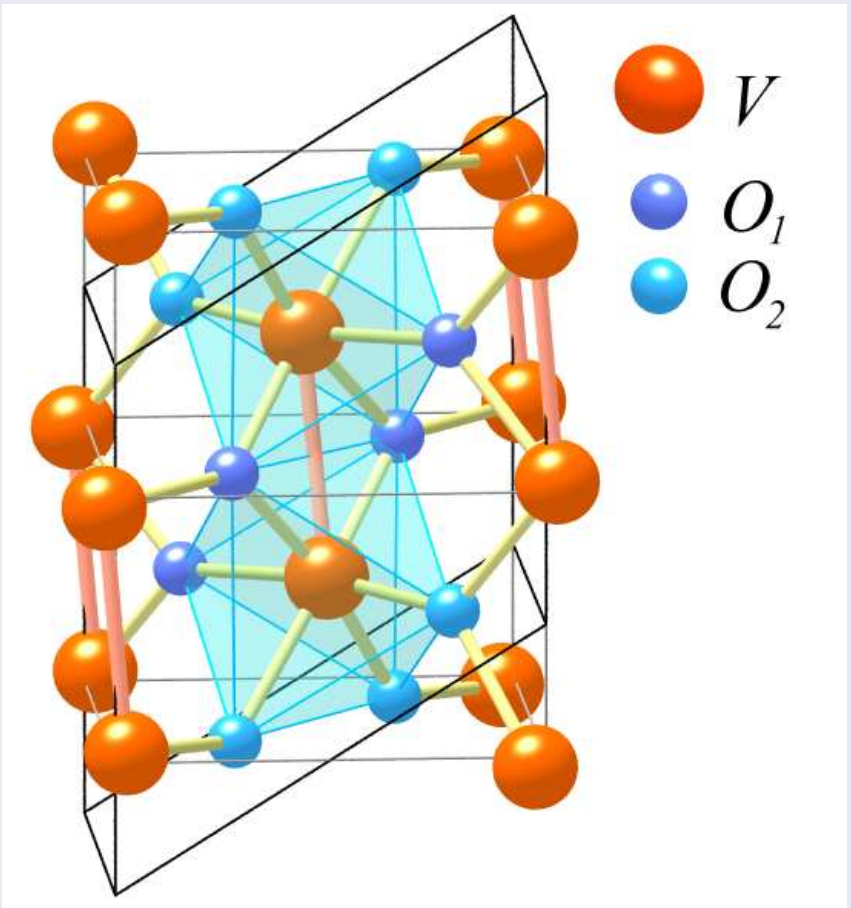

Metal-Insulator Transition of VO_2

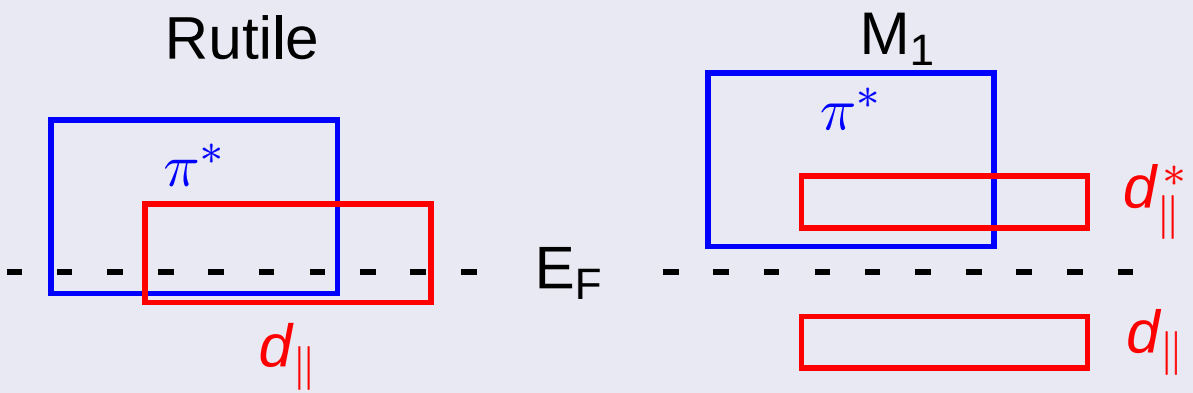

- Goodenough, 1960-1972
  - metal-metal dimerization $\| c_R \rightarrow$ splitting into $d_{\|}, d_{\|}^*$
  - antiferroelectric displacement $\perp c_R \rightarrow$ upshift of π^*
- Zylbersztejn and Mott, 1975
  - splitting of $d_{\|}$ by electronic correlations
  - upshift of π^* unscreenes $d_{\|}$ electrons

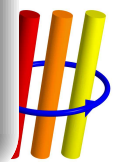

Metal-Insulator Transition of VO_2

Other Compounds

	d^0	d^1	d^2	d^3	d^4	d^5	d^6
3d	TiO_2 (S)	VO_2^* (M–S)	CrO_2 (F–M)	MnO_2 (AF–S)			
4d		NbO_2^* (M–S)	MoO_2^* (M)	TcO_2^* (M)	RuO_2 (M)	RhO_2 (M)	
5d		TaO_2 (?)	WO_2^* (M)	ReO_2^* (M)	OsO_2 (M)	IrO_2 (M)	PtO_2^* (M)

* deviations from rutile, M = metal, S = semiconductor
F/AF = ferro-/antiferromagnet

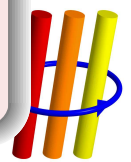

Metal-Insulator Transition of VO_2

Other Compounds

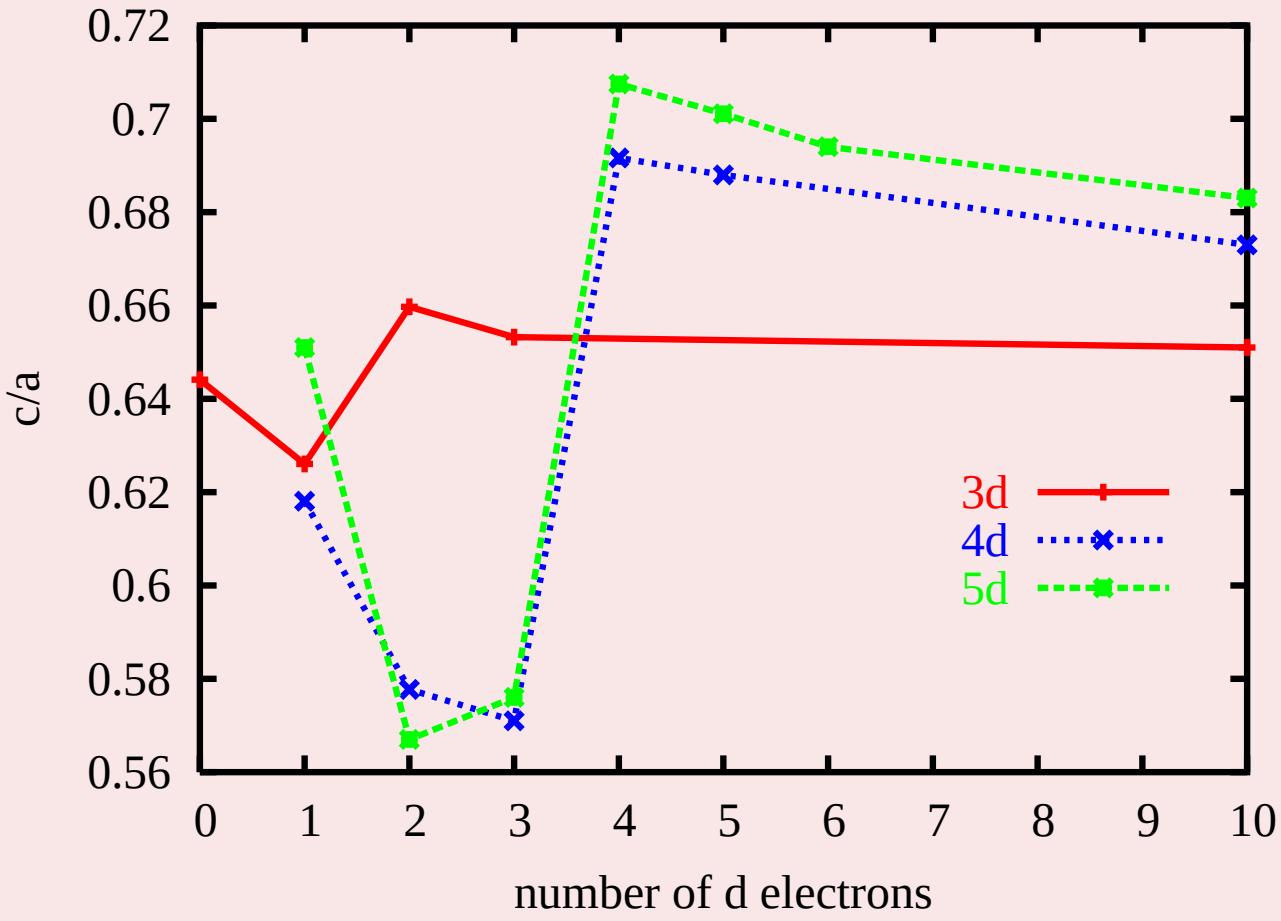

Metal-Insulator Transition of VO_2

Other Phases

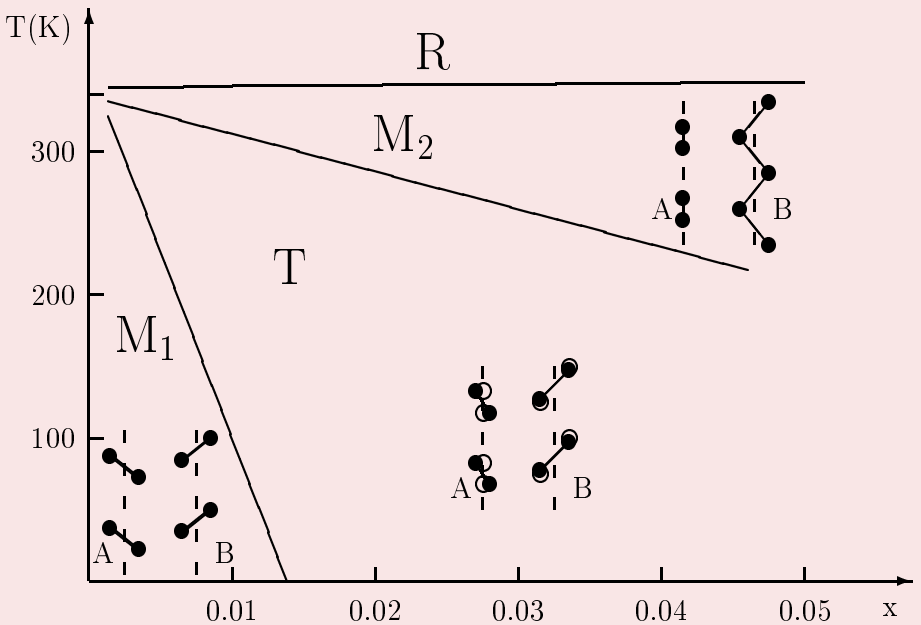

- doping with Cr, Al, Fe, Ga
- uniaxial pressure $\parallel \langle 110 \rangle$

$Cr_xV_{1-x}O_2$
Pouget, Launois, 1976

Electronic Structure in Detail

Rutile Structure

- molecular-orbital picture ✓
- octahedral crystal field
  $\Longrightarrow$ V 3*d* t_{2g}/e_g
- V 3*d*–O 2*p* hybridization

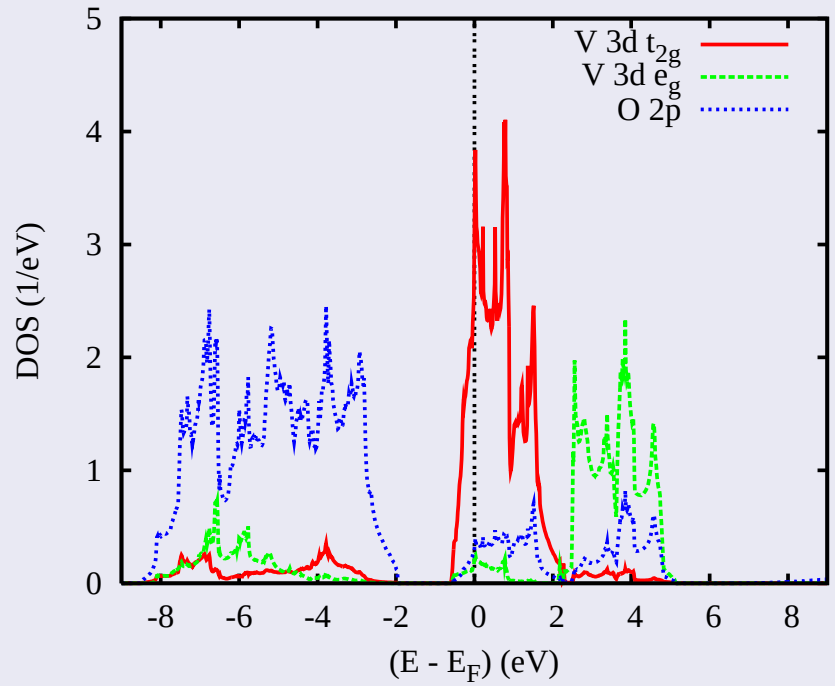

Ann. Phys. (Leipzig) **11**, 650 (2002)

Electronic Structure in Detail

Rutile Structure

- molecular-orbital picture ✓
- octahedral crystal field
  $\Longrightarrow$ V 3d t_{2g}/e_g
- V 3d–O 2p hybridization
- t_{2g} at E_F: $d_{x^2-y^2}$, d_{yz}, d_{xz}
- $n(d_{x^2-y^2}) \approx n(d_{yz}) \approx n(d_{xz})$

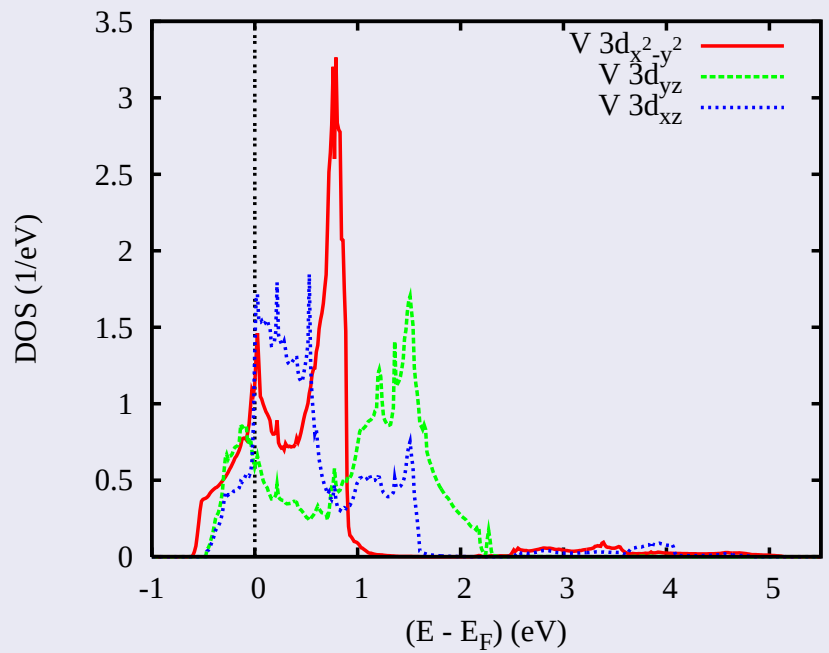

Ann. Phys. (Leipzig) **11**, 650 (2002)

Electronic Structure in Detail

$d_{||} = d_{x^2-y^2}$

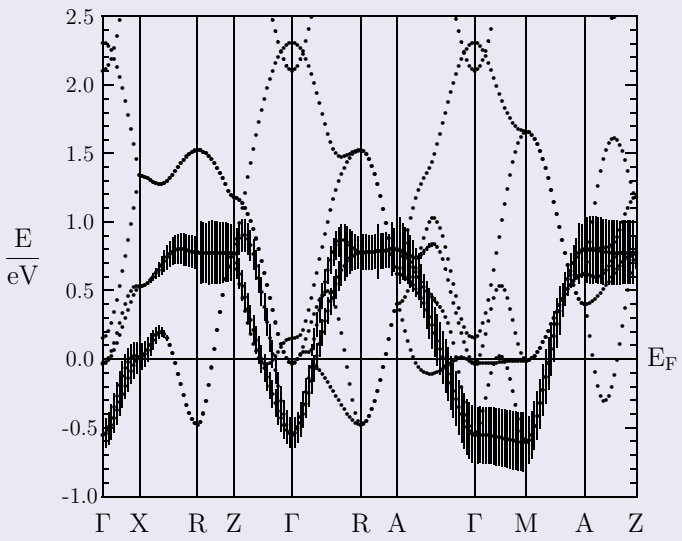

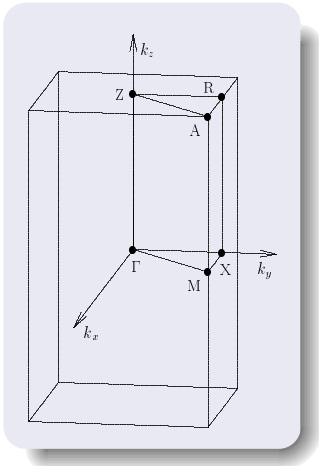

$\pi^* = (d_{yz}, d_{xz})$

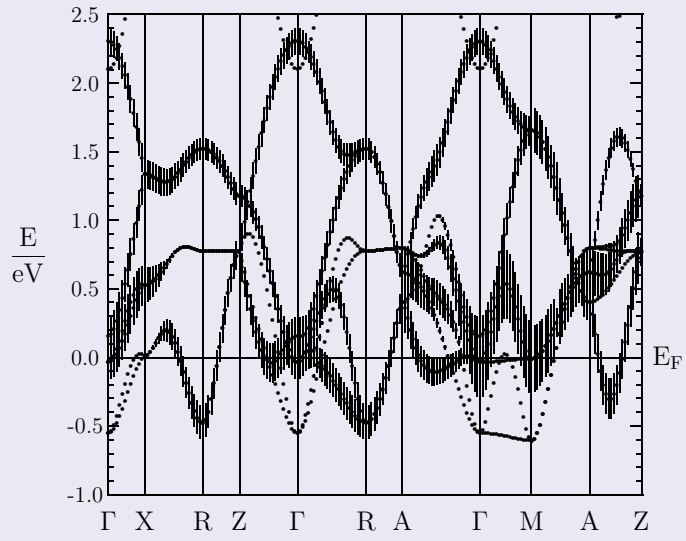

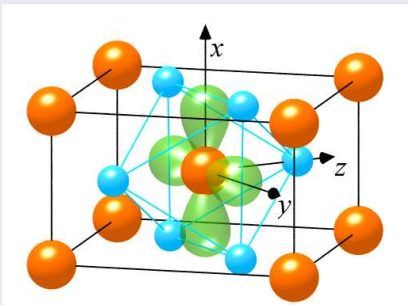

- 1D-dispersion of $d_{||}$ bands
- 3D-dispersion of π^* bands
- no hybridization between $d_{||}$ and π^*

Electronic Structure in Detail

Rutile Structure

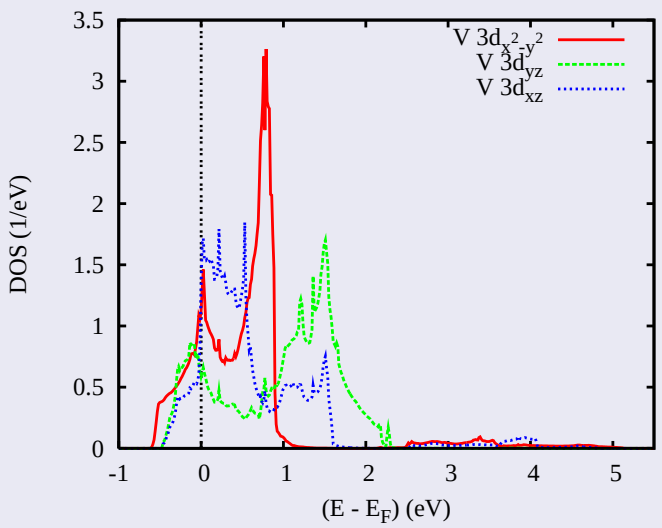

M_1 Structure

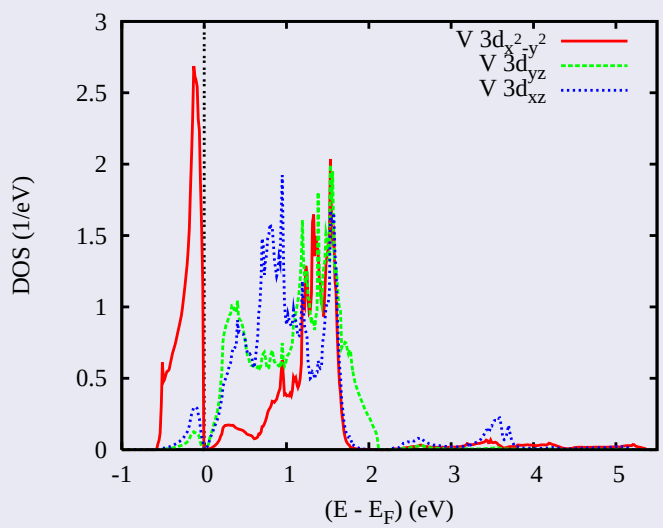

- bonding-antibonding splitting of $d_{\|}$ bands $\Longrightarrow$ embedded Peierls instability
- energetical upshift of π^* bands $\Longrightarrow$ orbital ordering
- optical band gap on the verge of opening

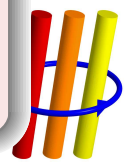

Electronic Structure in Detail

Rutile Structure

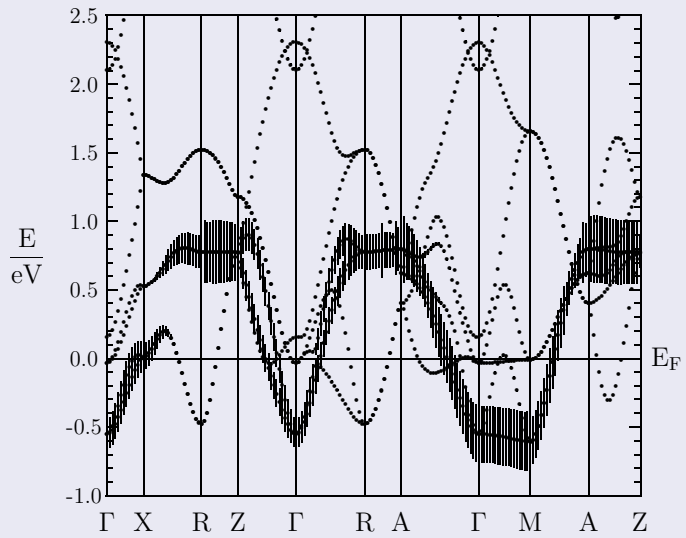

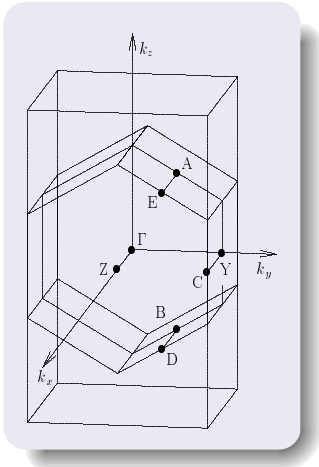

M_1 Structure

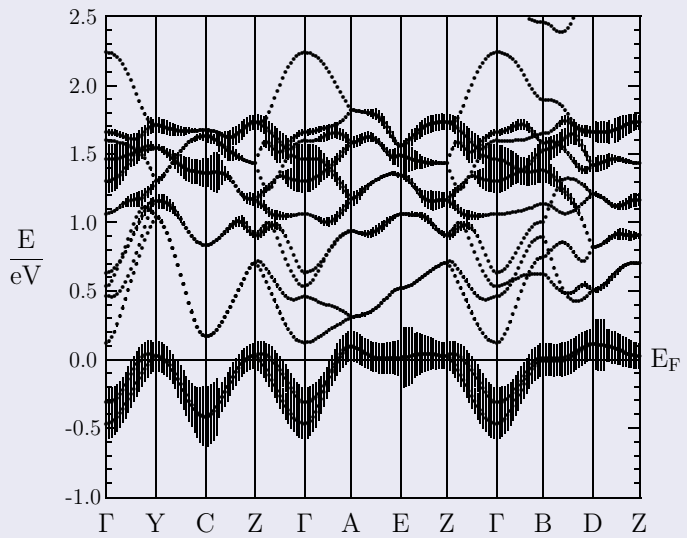

- bonding-antibonding splitting of $d_{||}$ bands $\Longrightarrow$ embedded Peierls instability
- energetical upshift of π^* bands $\Longrightarrow$ orbital ordering
- optical band gap on the verge of opening

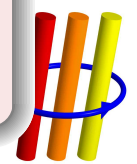

Further Investigations

Cluster-DMFT Calculations

- Rutile-VO_2
  - moderately correlated metal
- M_1-VO_2
  - correlations strong/weak on $d_{||}/\pi^*$
  - optical band gap of 0.6 eV
- Phase Transition
  - "correlation-assisted Peierls transition"

S. Biermann, A. Poteryaev, A. I. Lichtenstein, A. Georges
PRL **94**, 026404 (2005)

Further Investigations

Rutile

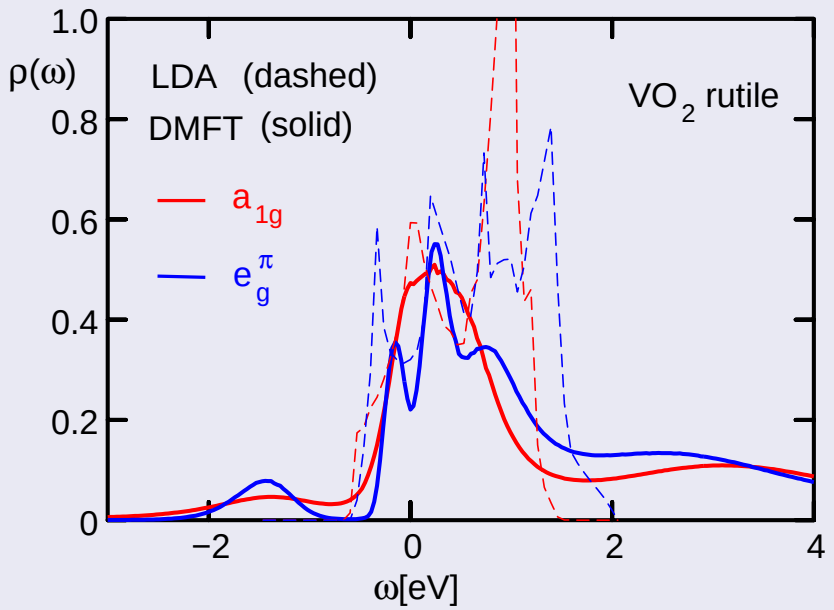

M_1

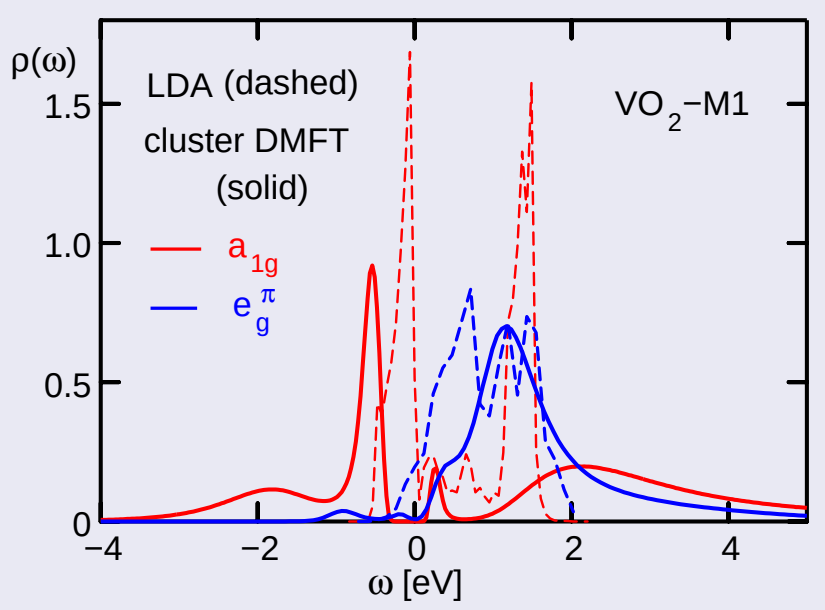

Transition-Metal Dioxides: Partial d t_{2g} DOS

VO_2 ($3d^1$)

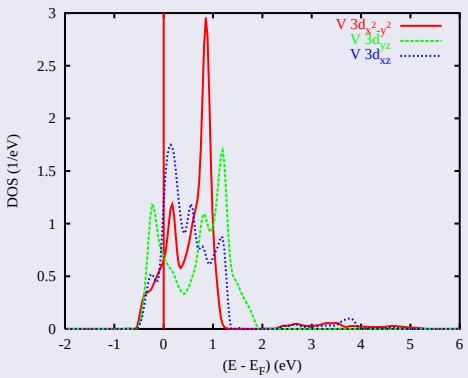

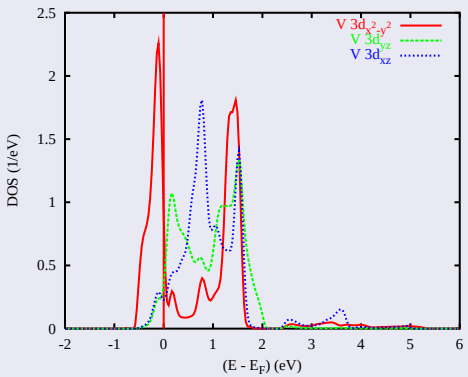

NbO_2 ($4d^1$)

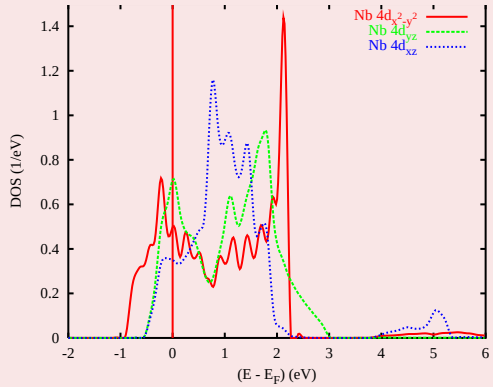

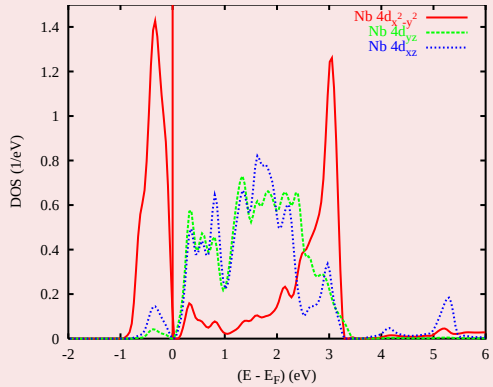

MoO_2 ($4d^2$)

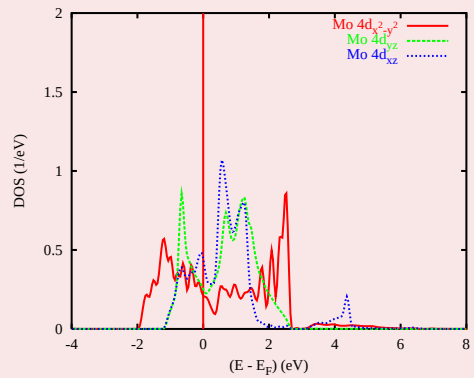

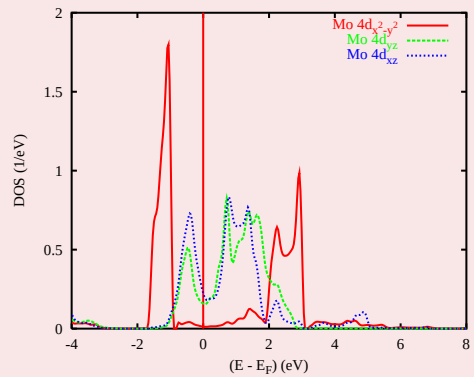

Transition-Metal Dioxides: Partial d t_{2g} DOS

VO_2 ($3d^1$)

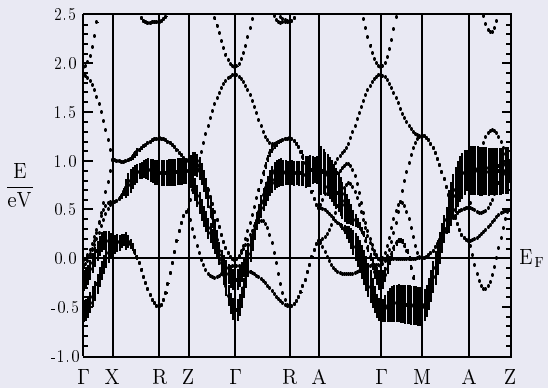

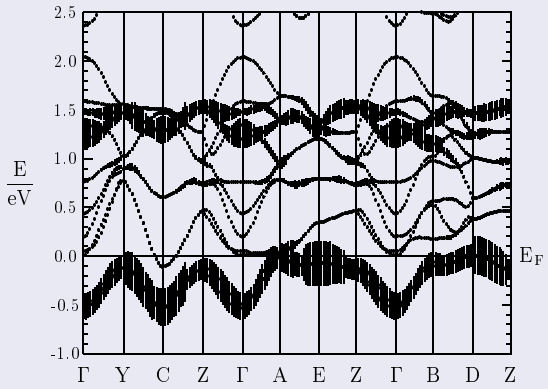

NbO_2 ($4d^1$)

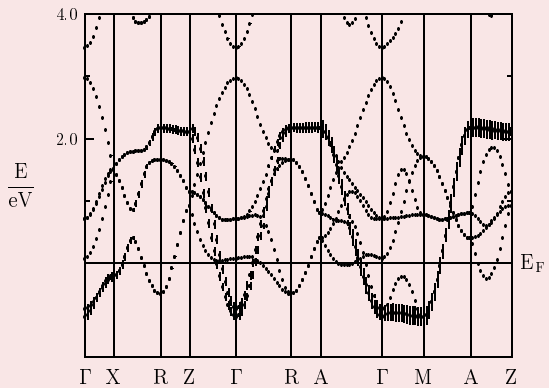

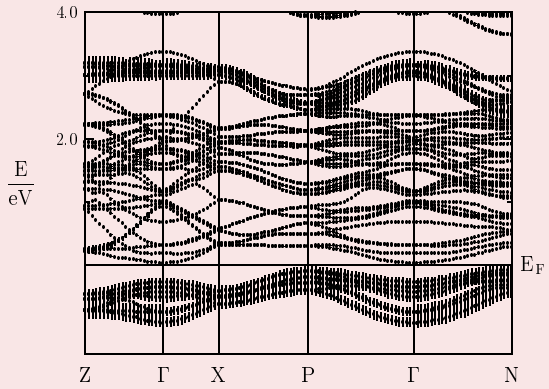

MoO_2 ($4d^2$)

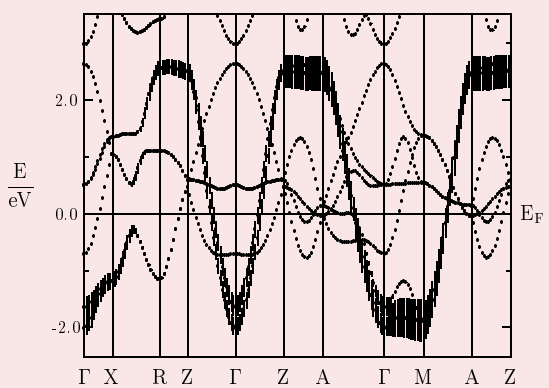

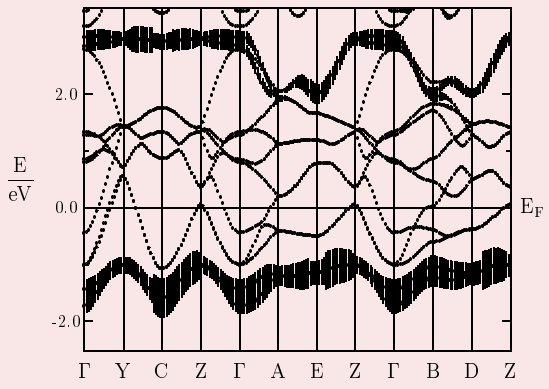

Electronic Structure in Detail: M_2-VO_2

dimerized chains

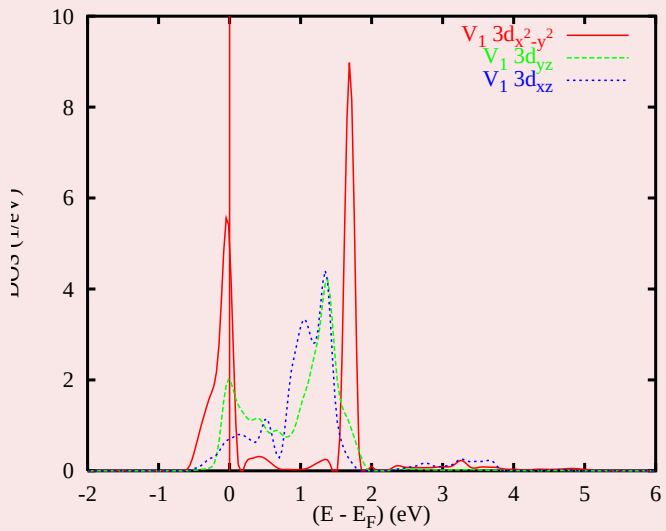

zigzag chains

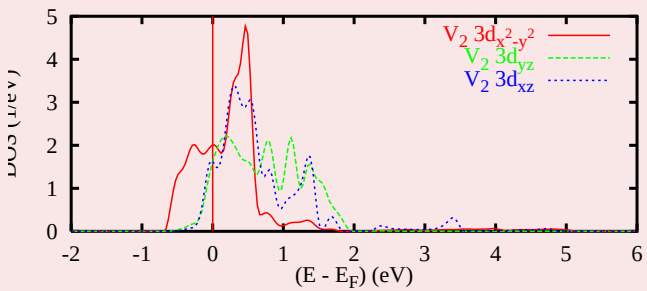

Electronic Structure in Detail: M_2-VO_2 (AF)

dimerized chains

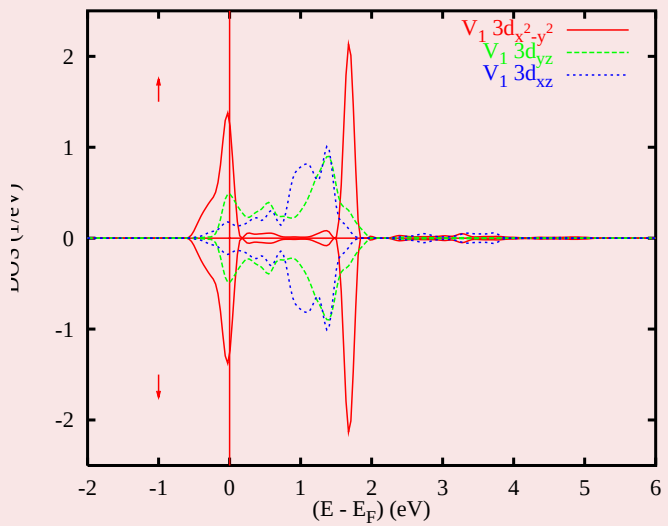

zigzag chains

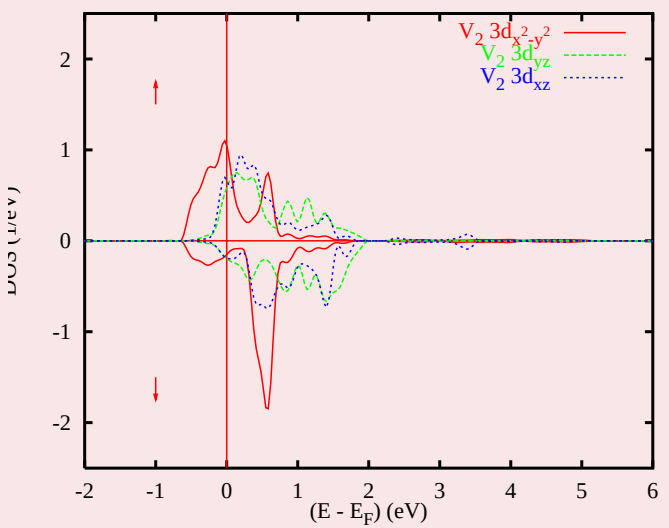

Critical review of the Local Density Approximation

Limitations and Beyond

- Self-interaction cancellation in $v_{Hartree} + v_x$ violated
- Repair using exact Hartree-Fock exchange functional $\longrightarrow$ class of hybrid functionals
  - PBE0

$$E_{xc}^{PBE0} = \frac{1}{4}E_x^{HF} + \frac{3}{4}E_x^{PBE} + E_c^{PBE}$$

  - HSE03, HSE06

$$E_{xc}^{HSE} = \frac{1}{4}E_x^{HF,sr,\mu} + \frac{3}{4}E_x^{PBE,sr,\mu} + E_x^{PBE,lr,\mu} + E_c^{PBE}$$

based on decomposition of Coulomb kernel

$$\frac{1}{r} = S_\mu(r) + L_\mu(r) = \frac{\mathrm{erfc}(\mu r)}{r} + \frac{\mathrm{erf}(\mu r)}{r}$$

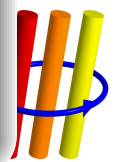

Critical review of the Local Density Approximation

Limitations and Beyond

- Self-interaction cancellation in $v_{Hartree} + v_x$ violated
- Repair using exact Hartree-Fock exchange functional
  $\longrightarrow$ class of hybrid functionals

GGA

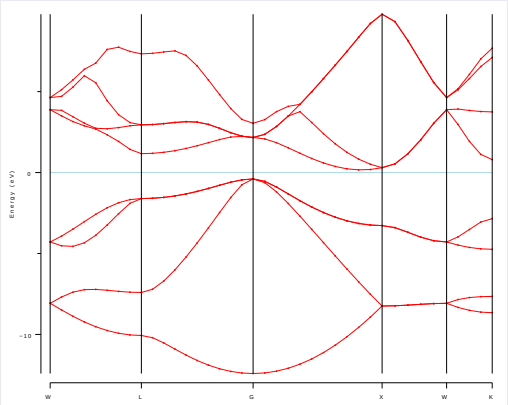

Si bandgap

- exp: 1.11 eV
- GGA: 0.57 eV
- HSE: 1.15 eV

HSE

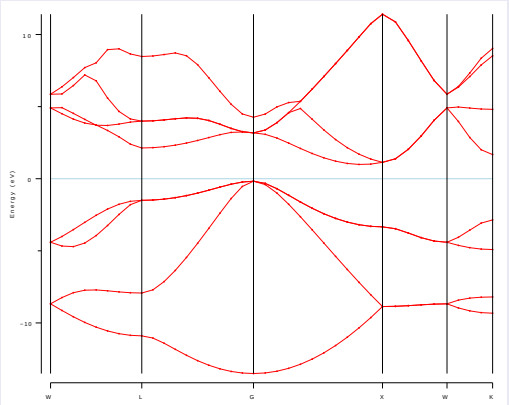

Critical review of the Local Density Approximation

Limitations and Beyond

- Self-interaction cancellation in $v_{Hartree} + v_x$ violated
- Repair using exact Hartree-Fock exchange functional
  $\longrightarrow$ class of hybrid functionals

GGA

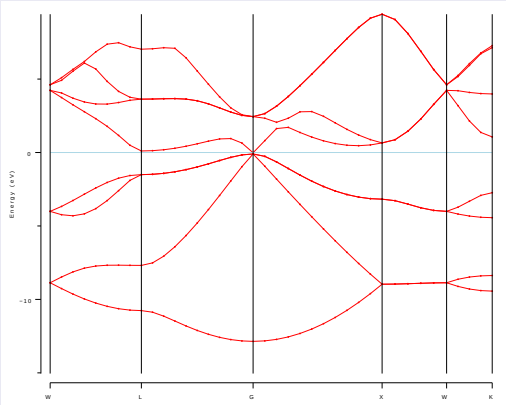

Ge bandgap

- exp: 0.67 eV
- GGA: 0.09 eV
- HSE: 0.66 eV

HSE

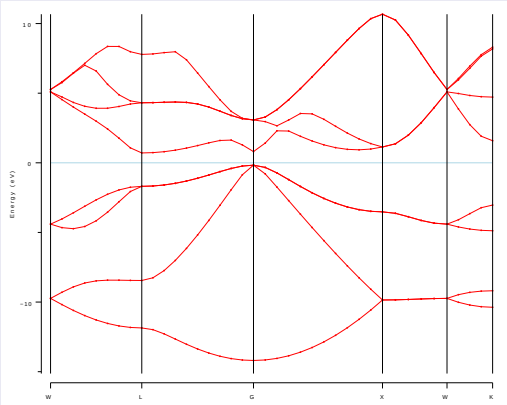

Critical review of the Local Density Approximation

Calculated vs. experimental bandgaps

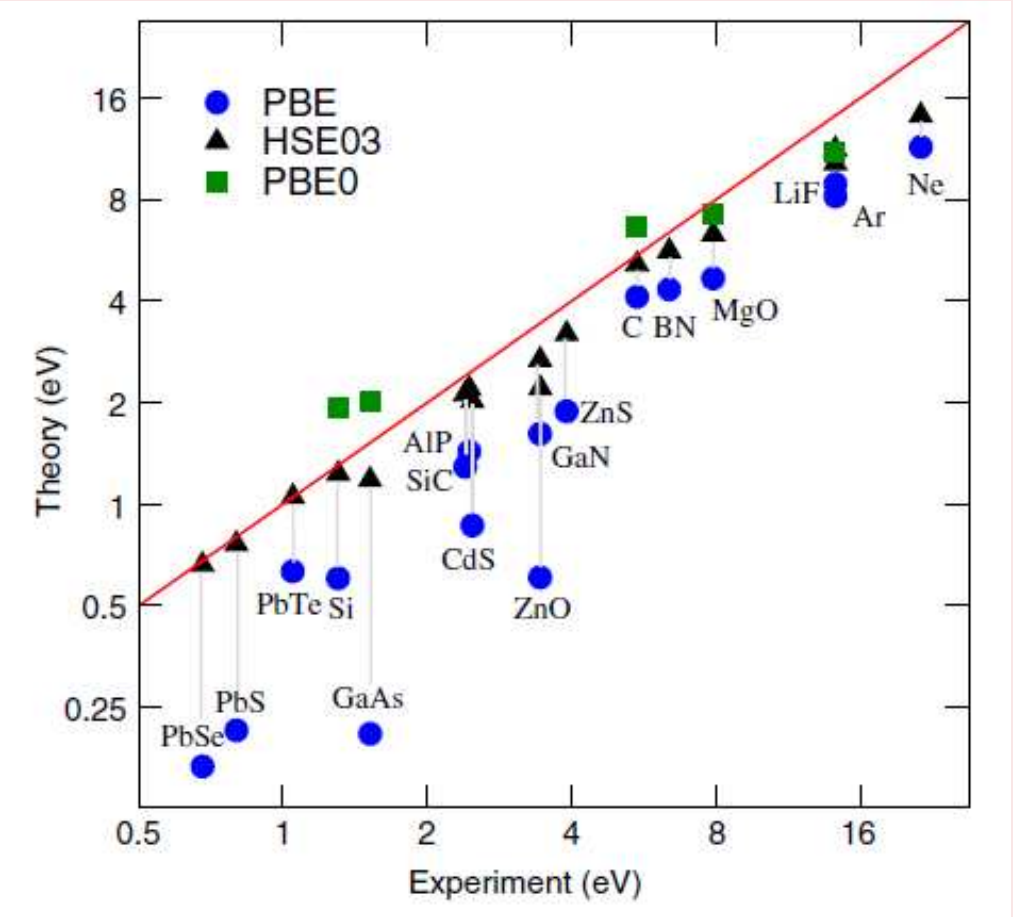

$SrTiO_3$

GGA

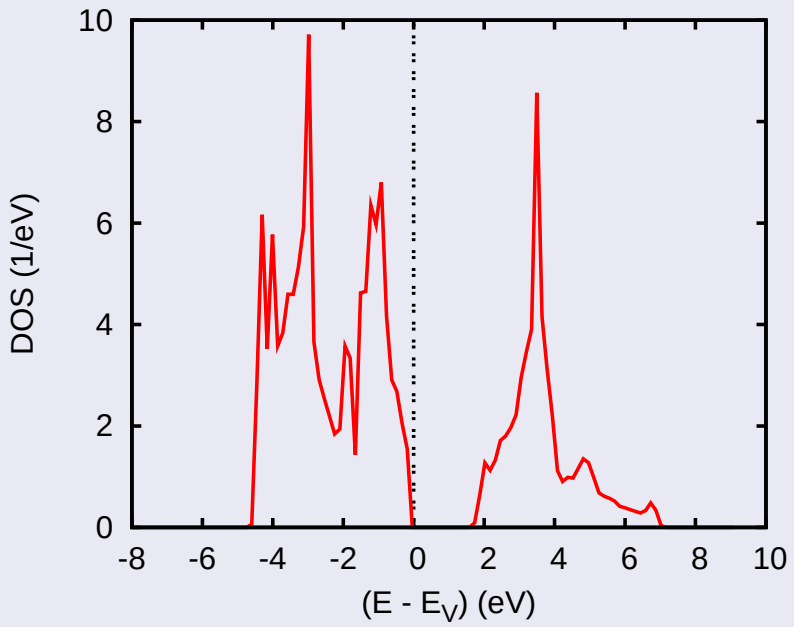

Bandgap

GGA: $\approx 1.6\,eV$, exp.: $3.2\,eV$

$SrTiO_3$

GGA

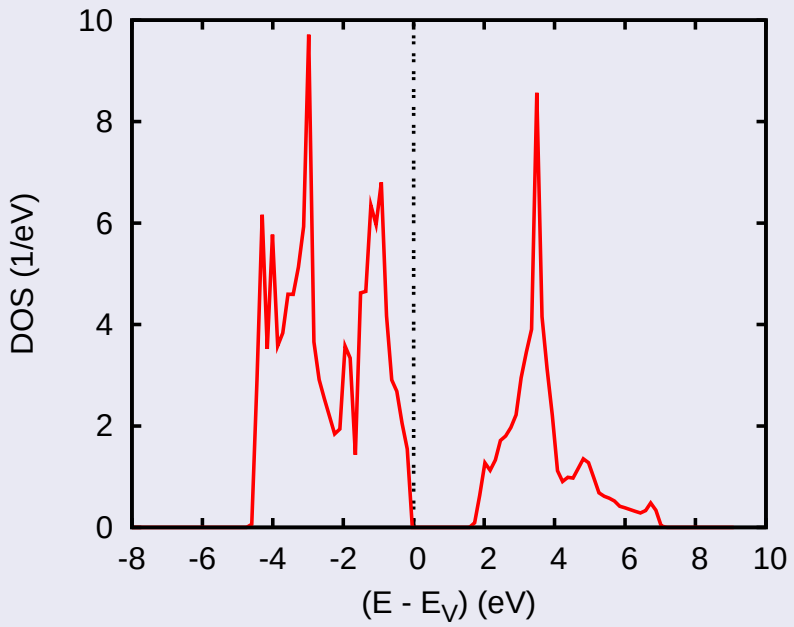

HSE

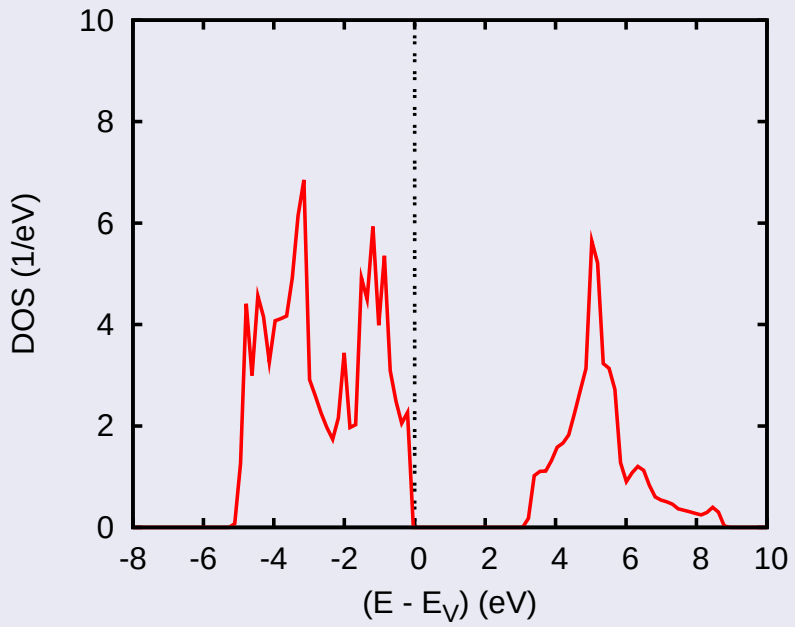

Bandgap

GGA: $\approx 1.6\,eV$, HSE: $\approx 3.1\,eV$, exp.: $3.2\,eV$

$LaAlO_3$

GGA

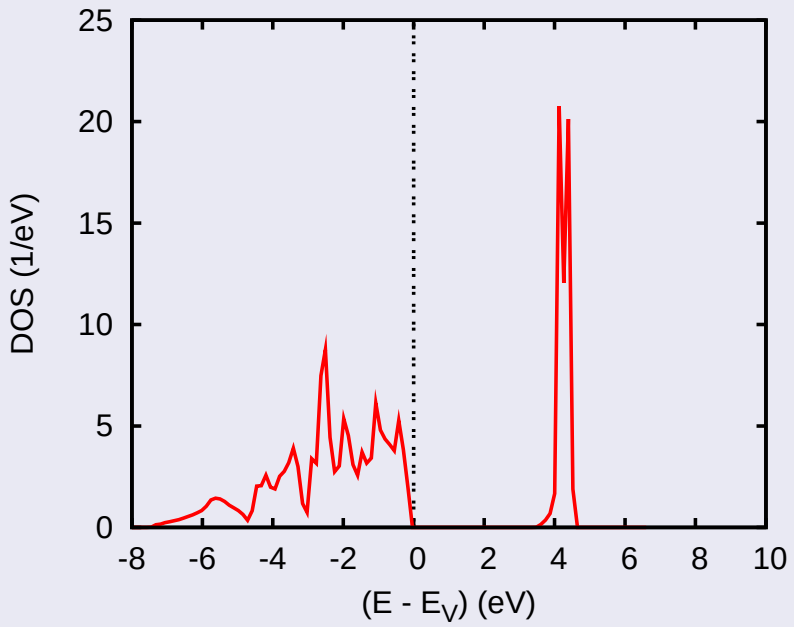

Bandgap

GGA: $\approx 3.5\,eV$, exp.: $5.6\,eV$

$LaAlO_3$

GGA

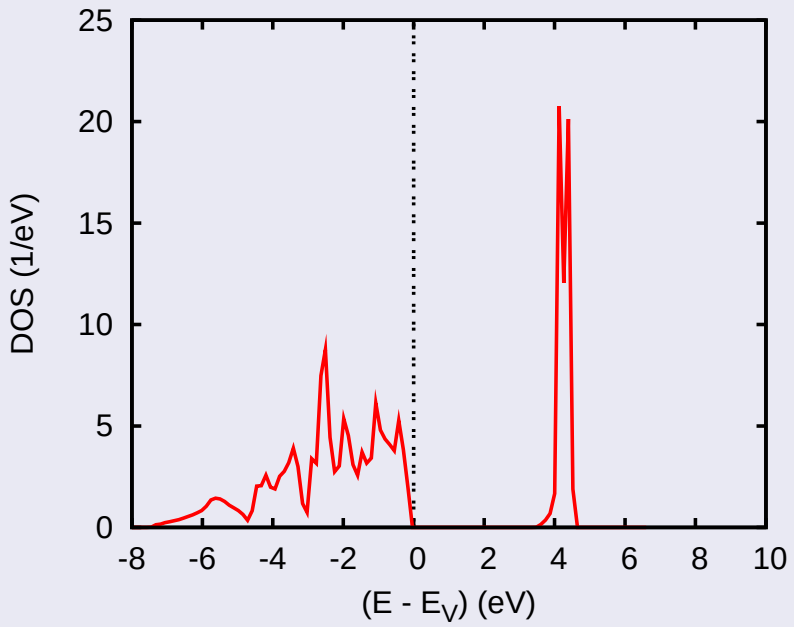

HSE

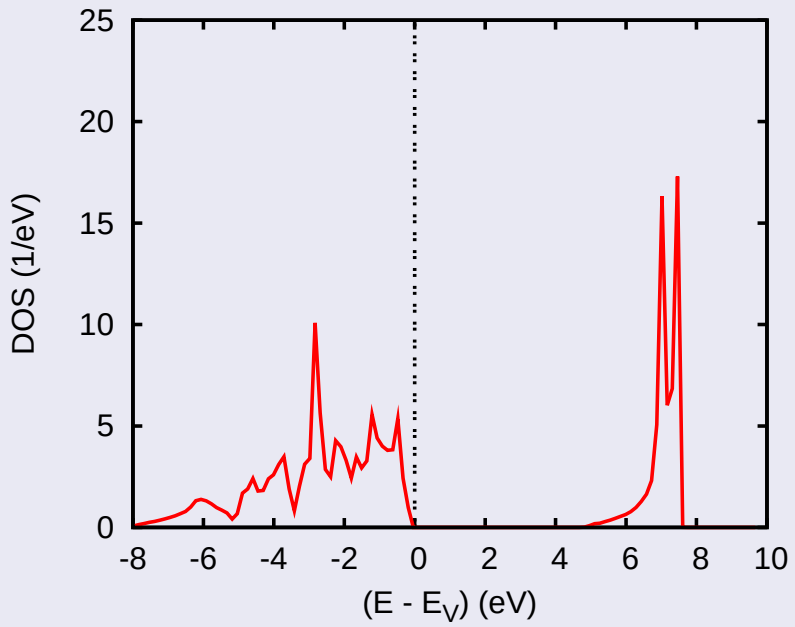

Bandgap

GGA: $\approx 3.5\,eV$, HSE: $\approx 5.0\,eV$, exp.: $5.6\,eV$

2D Electron Gas at $LaAlO_3$-$SrTiO_3$ Interface

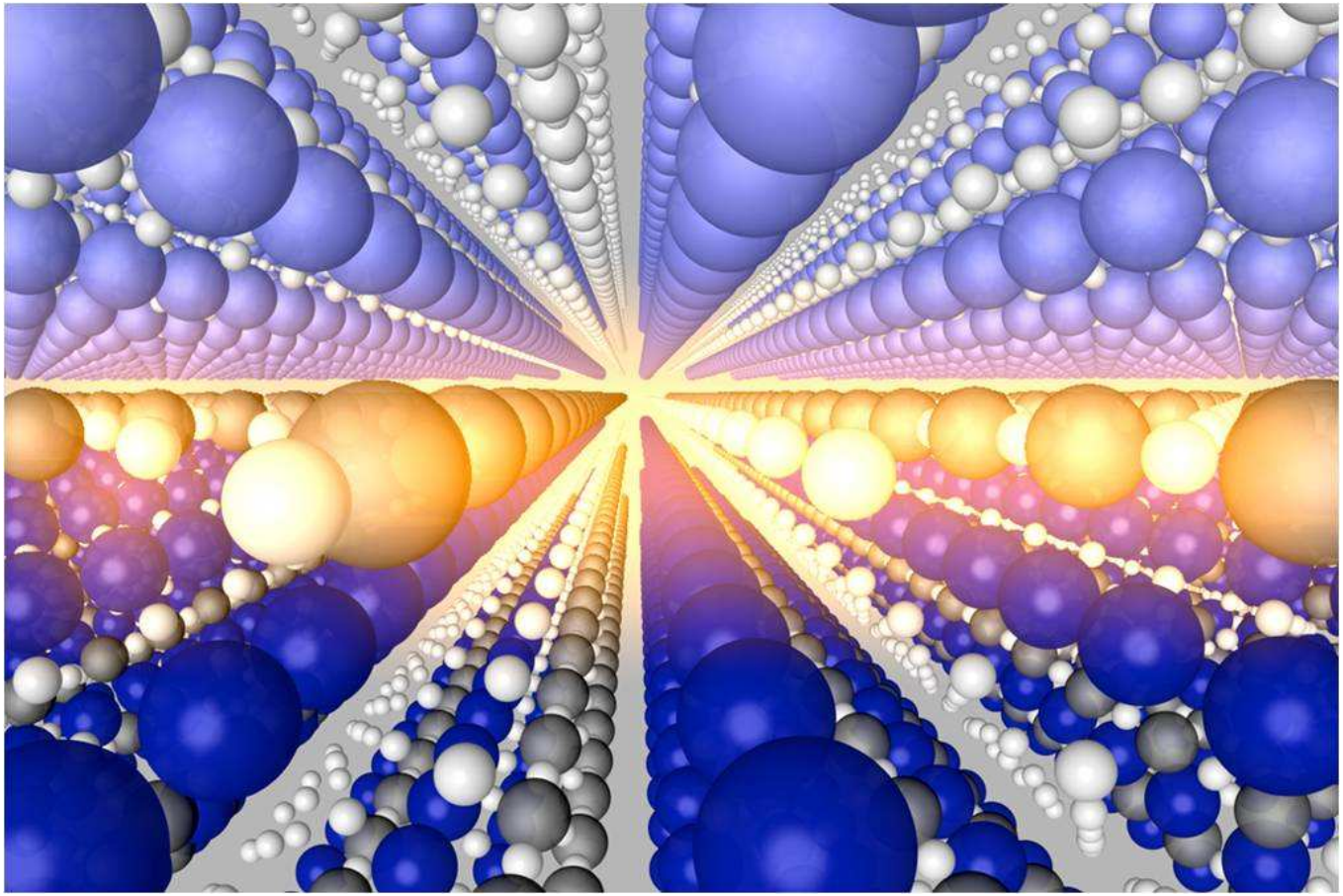

2D Electron Gas at $LaAlO_3$-$SrTiO_3$ Interface

Issues

- Role of electronic correlations?
  - $SrTiO_3$, $LaAlO_3$: band insulators
  - $SrTiO_3/LaAlO_3$ interface: MIT (# $LaAlO_3$ layers)
  - magnetic properties of the interface
  - superconductivity below $\approx 200\,\mathrm{mK}$
- What is the origin of the 2-DEG?
  - intrinsic mechanism?
  - defect-doping?

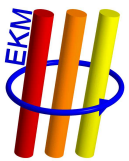

2D Electron Gas at $LaAlO_3$-$SrTiO_3$ Interface

Insulator-Metal Transition

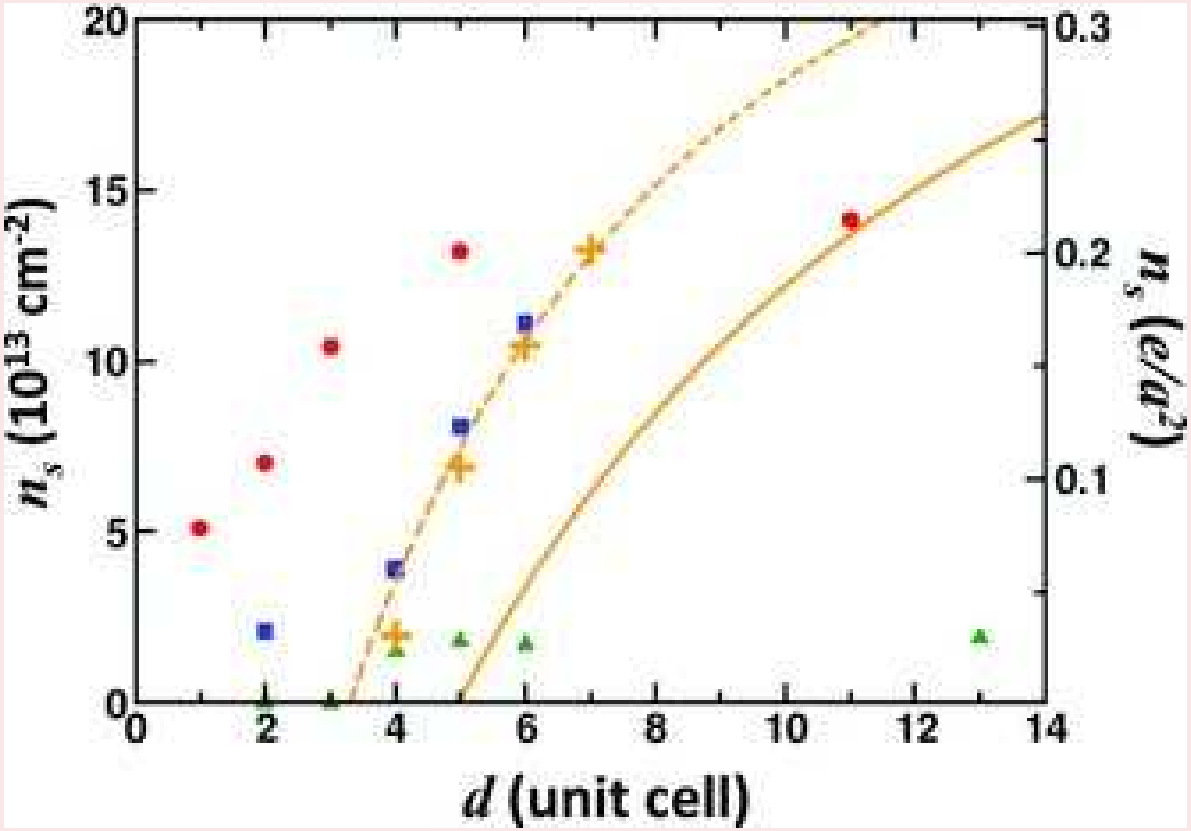

Chen, Kolpak, Ismail-Beigi, Adv. Mater. **22**, 2881 (2010)

Slab Calculations for the $LaAlO_3$-$SrTiO_3$ Interface

Structural setup of calculations

- central region: 5 layers $SrTiO_3$, TiO_2-terminated
- sandwiches: 2 to 5 layers $LaAlO_3$, AlO_2 surface
- vacuum region $\approx$ 20 Å
- inversion symmetry
- lattice constant of $SrTiO_3$ from GGA (3.944 Å)

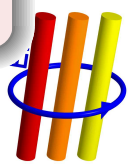

Slab Calculations for the $LaAlO_3$-$SrTiO_3$ Interface

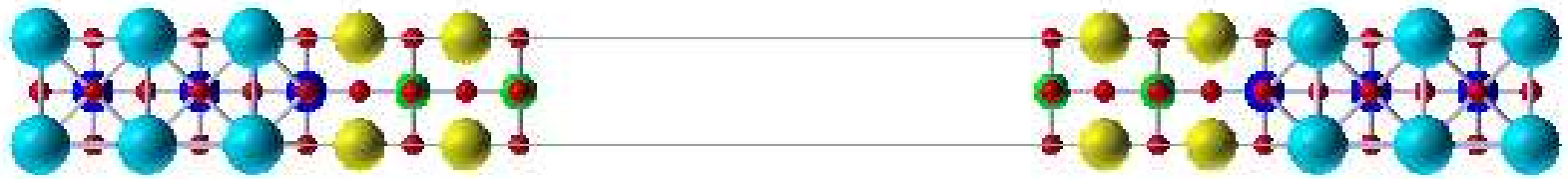

Calculational method

- Vienna Ab Initio Simulation Package (VASP)
- GGA-PBE
- Steps:
  1. optimization of $SrTiO_3$ lattice constant
  2. slab calculations
     - full relaxation of all atomic positions
     - $5 \times 5 \times 1$ **k**-points
     - Γ-centered **k**-mesh
     - Methfessel-Paxton BZ-integration

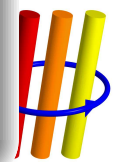

Slab Calculations for the $LaAlO_3$-$SrTiO_3$ Interface

Ideal

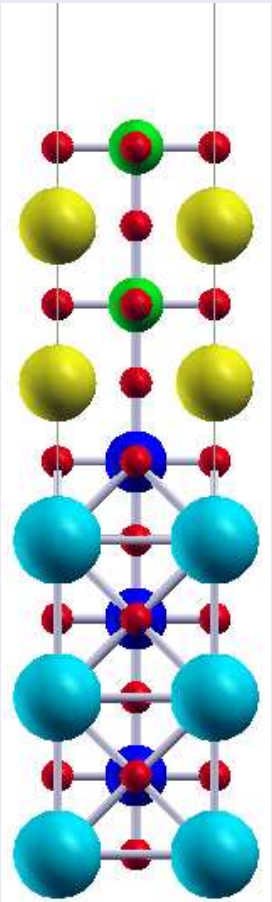

Structural relaxation

- AlO_2 surface layers
  - strong inward relaxation
  - weak buckling
- LaO layers
  - strong buckling
- AlO_2 subsurface layers
  - buckling
- TiO_2 interface layers
  - small outward relaxation

Optimized

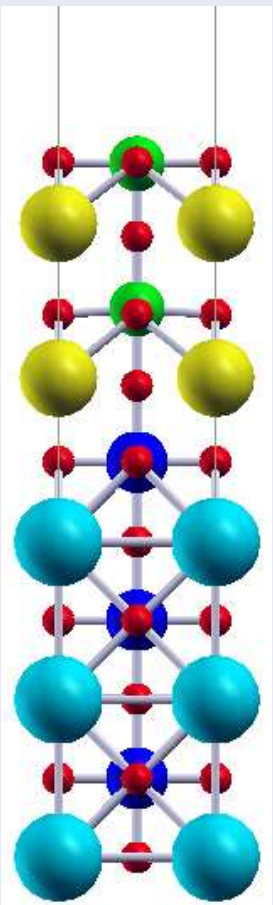

Slab Calculations for the $LaAlO_3$-$SrTiO_3$ Interface

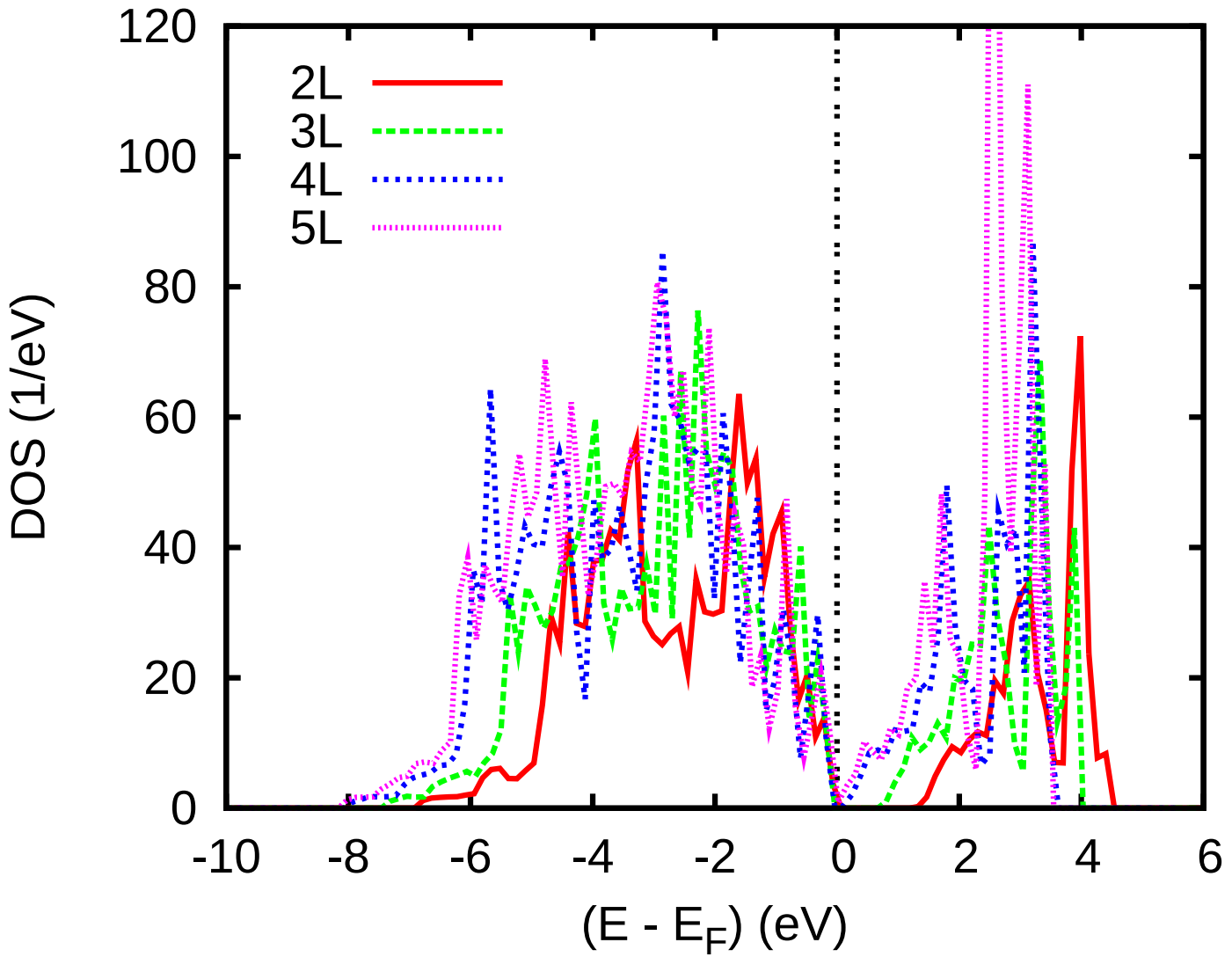

New Calculations: GGA vs. HSE

Rutile Structure GGA

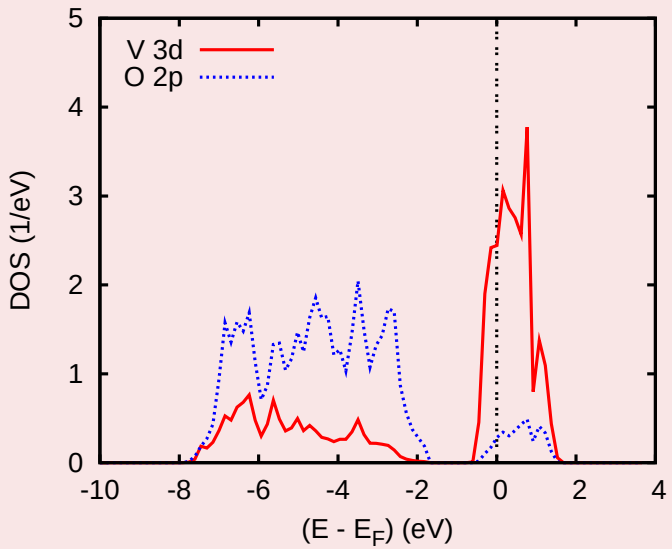

Rutile Structure HSE

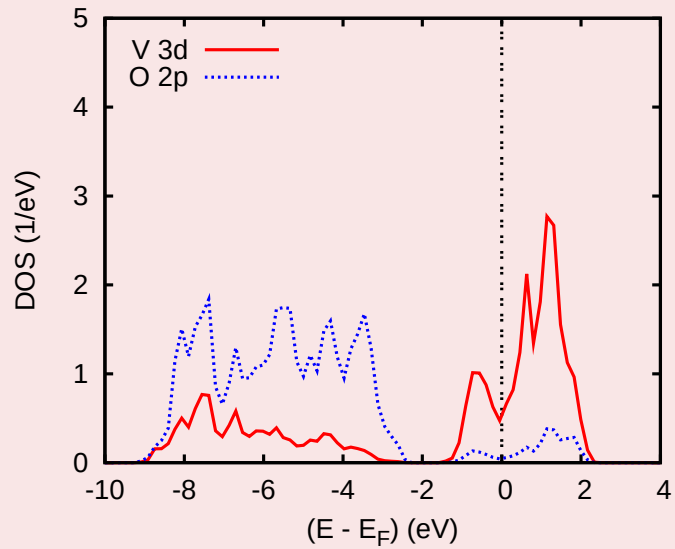

Rutile Structure: GGA $\Longrightarrow$ HSE

- broadening of O $2p$ and V $3d$ t_{2g}(!) bands
- splitting within V $3d$ t_{2g} bands

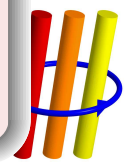

New Calculations: GGA vs. HSE

M_1 Structure GGA

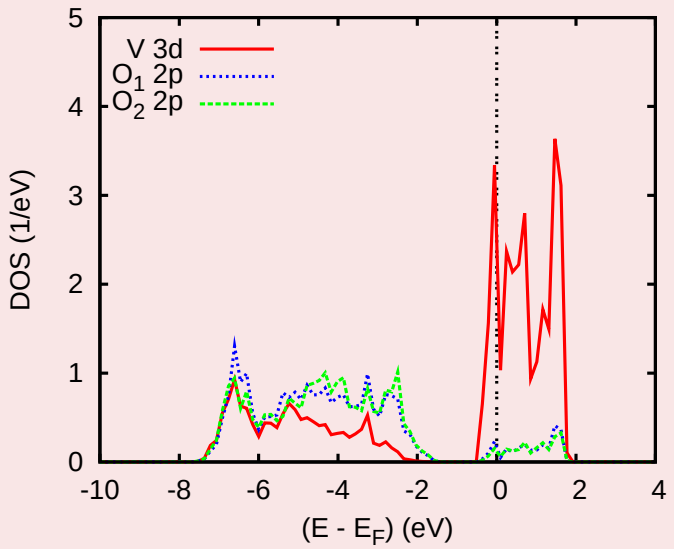

M_1 Structure HSE

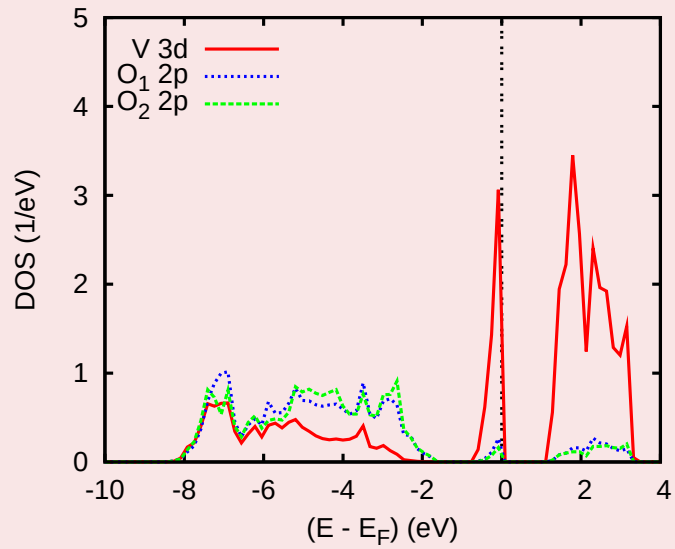

M_1 Structure: GGA $\Longrightarrow$ HSE

- splitting of $d_{||}$ bands, upshift of π^* bands
- optical bandgap of ≈ 1 eV

New Calculations: GGA vs. HSE

M_1 Structure GGA

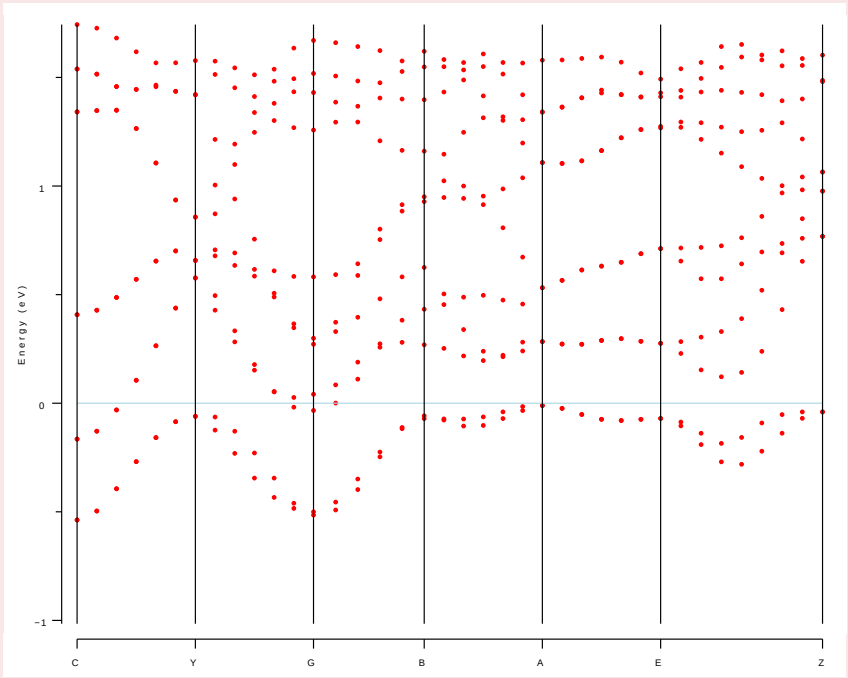

M_1 Structure HSE

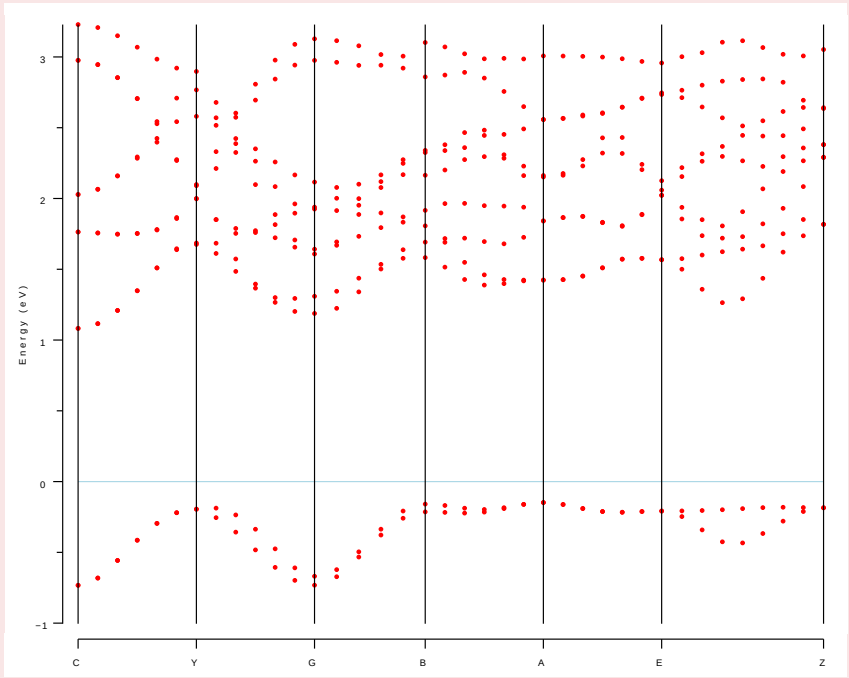

M_1 Structure: GGA $\Longrightarrow$ HSE

- splitting of $d_{\|}$ bands, upshift of π^* bands
- optical bandgap of ≈ 1 eV

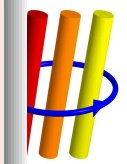

New Calculations: GGA vs. HSE

M_2 Structure GGA

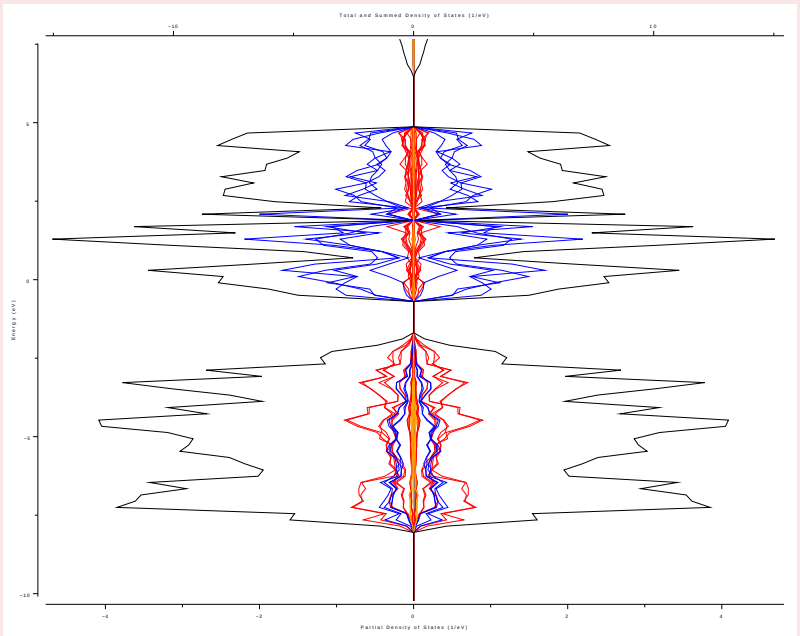

M_2 Structure HSE

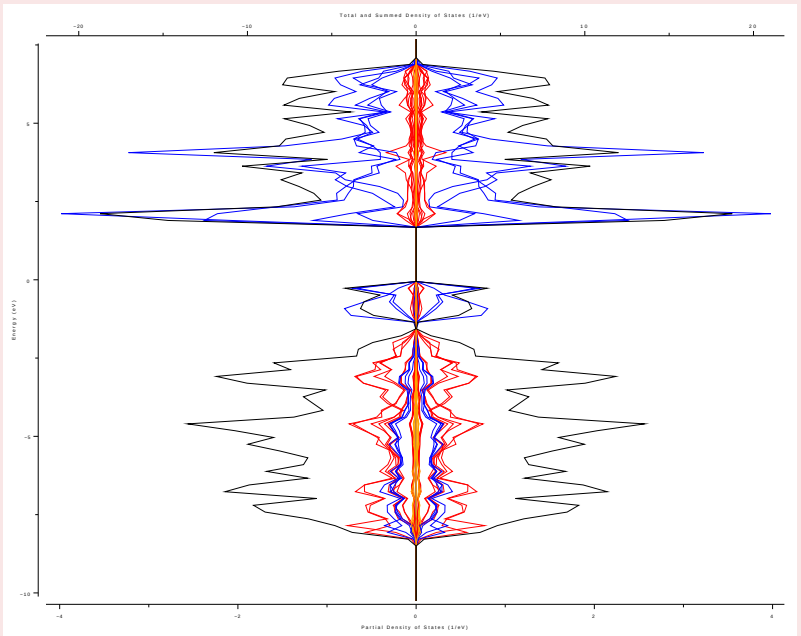

M_2 Structure: GGA $\Longrightarrow$ HSE

- localized magentic moment of 1 μ_B
- optical bandgap of $\approx$ 1.6 eV

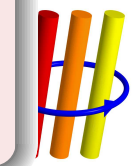

Unified Picture

Rutile-Related Transition-Metal Dioxides

VO_2 ($3d^1$), NbO_2 ($4d^1$), MoO_2 ($4d^2$)
(WO_2 ($5d^2$), TcO_2 ($4d^3$), ReO_2 ($5d^3$))

- instability against similar local distortions
  - metal-metal dimerization $\parallel c_R$
  - antiferroelectric displacement $\perp c_R$
- („accidental“) metal-insulator transition of the d^1-members

VE *et al.*, J. Phys.: CM **12**, 4923 (2000)
VE, Ann. Phys. **11**, 650 (2002)
VE, EPL **58**, 851 (2002)
J. Moosburger-Will *et al.*, PRB **79**, 115113 (2009)

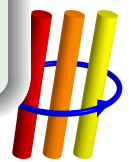

From VO_2 to ...

... CrO_2: Applications

- half-metallic ferromagnet
- $T_C \approx 391\,K$

Partial DOS

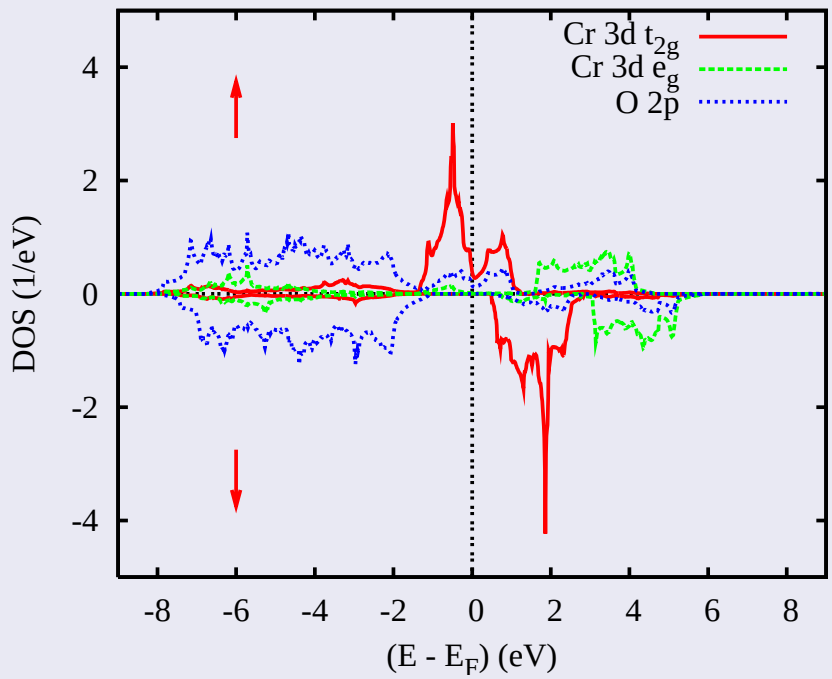

J. Phys. I France **2**, 315 (1992)
J. Phys. I France **4**, 1199 (1994)

From VO_2 to ...

... CrO_2: Applications

- half-metallic ferromagnet
- $T_C \approx 391\,K$

Spin Density

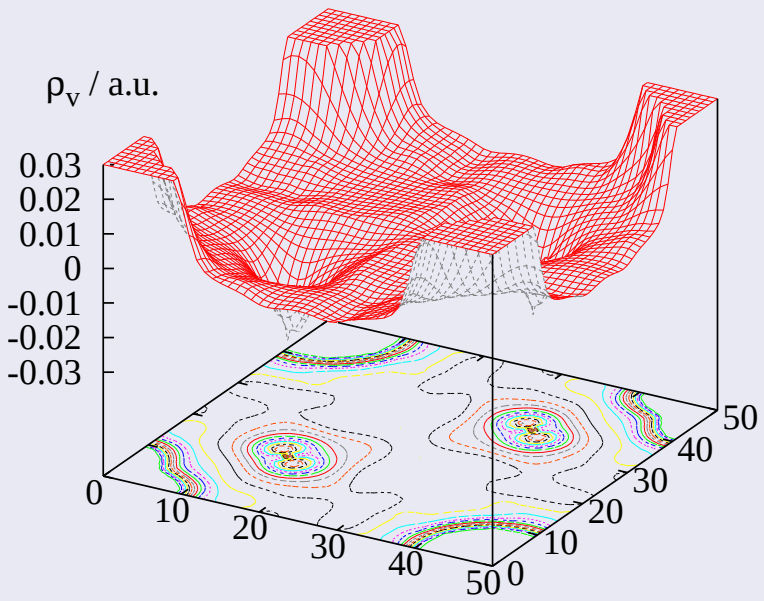

Partial DOS

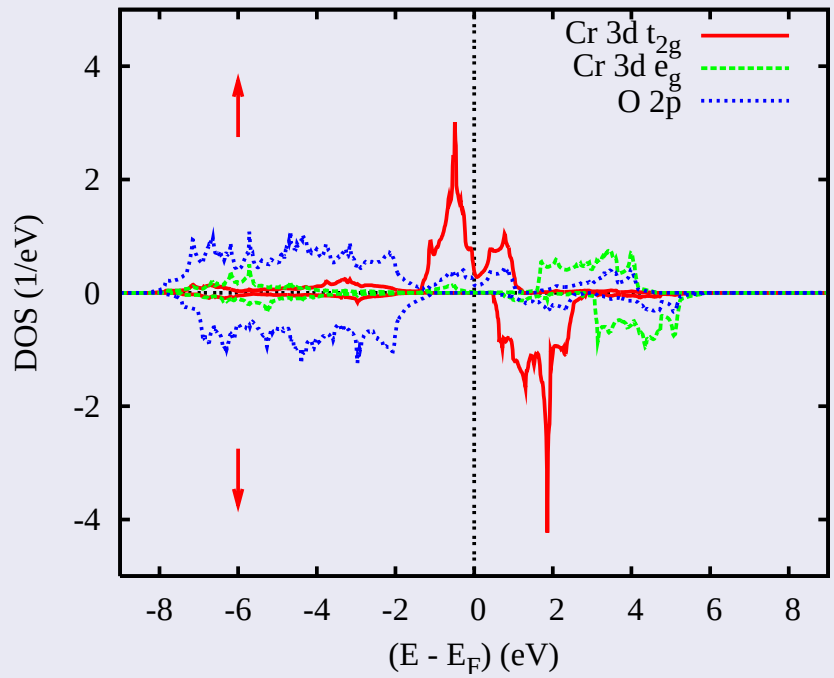

J. Phys. I France **2**, 315 (1992)
J. Phys. I France **4**, 1199 (1994)

From VO_2 to ...

... V_2O_3: Magnéli-Phases

$$V_nO_{2n-1} = V_2O_3 + (n-2)VO_2$$

- $n \to \infty$: VO_2
- $n = 2$: V_2O_3
- variation of *d*-band filling
- metal-insulator transitions
- structural transformations
- rutile-type slabs of thickness $\sim n$
- corundum-like shear planes

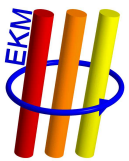

From VO_2 to ...

... V_2O_3: Magnéli-Phases

$V_nO_{2n-1} = V_2O_3 + (n-2)VO_2$

- $n \to \infty$: VO_2
- $n = 2$: V_2O_3
- variation of *d*-band filling
- metal-insulator transitions
- structural transformations
- rutile-type slabs of thickness $\sim n$
- corundum-like shear planes

VO_2 ($n \to \infty$)

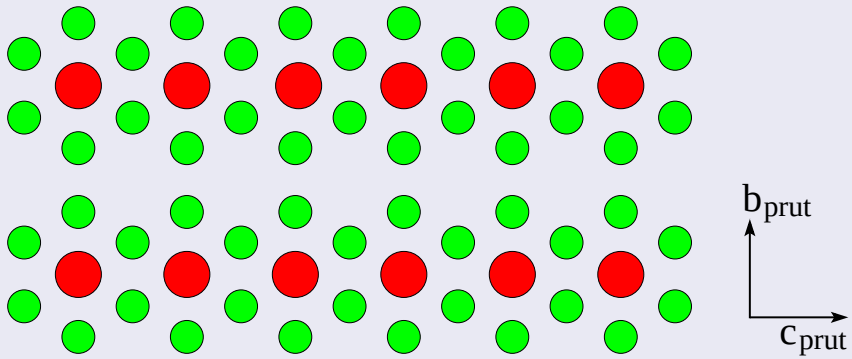

- O octahedra
- occupied by V
- Magnéli phase characterized by V-chain length n

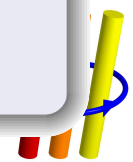

From VO_2 to ...

... V_2O_3: Magnéli-Phases

$V_nO_{2n-1} = V_2O_3 + (n-2)VO_2$

- $n \to \infty$: VO_2
- $n = 2$: V_2O_3
- variation of *d*-band filling
- metal-insulator transitions
- structural transformations
- rutile-type slabs of thickness $\sim n$
- corundum-like shear planes

V_4O_7 ($n = 4$)

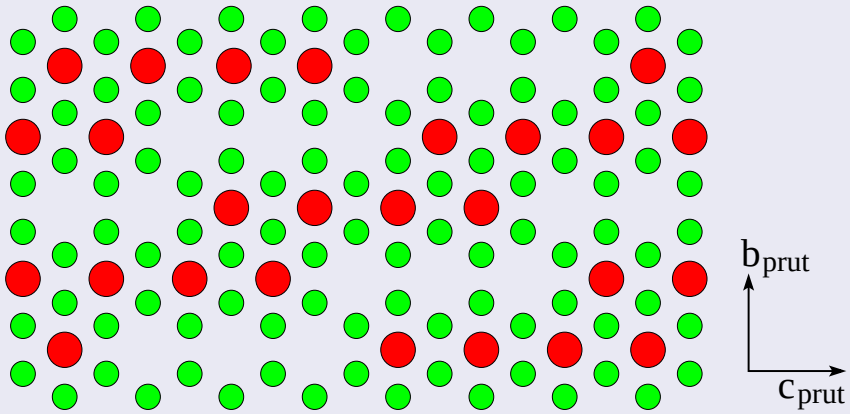

- O octahedra
- occupied by V
- Magnéli phase characterized by V-chain length n

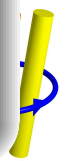

From VO_2 to ...

... V_2O_3: Magnéli-Phases

$V_nO_{2n-1} = V_2O_3 + (n-2)VO_2$

- $n \to \infty$: VO_2
- $n = 2$: V_2O_3
- variation of *d*-band filling
- metal-insulator transitions
- structural transformations
- rutile-type slabs of thickness $\sim n$
- corundum-like shear planes

V_2O_3 ($n = 2$)

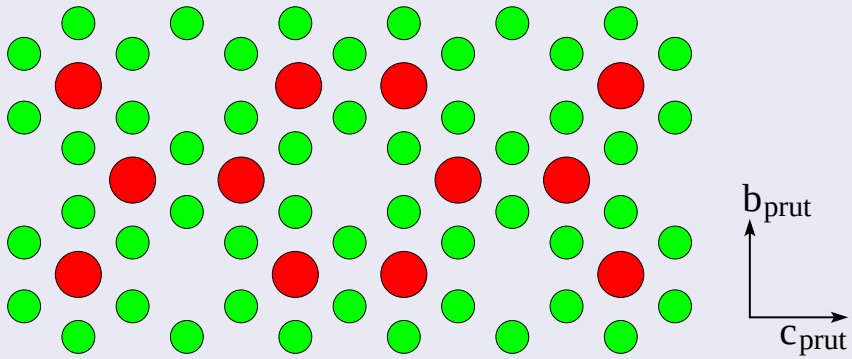

- O octahedra
- occupied by V
- Magnéli phase characterized by V-chain length n

From VO_2 to ...

... V_2O_3: Magnéli-Phases

$V_nO_{2n-1} = V_2O_3 + (n-2)VO_2$

- $n \to \infty$: VO_2
  - one-dimensional
  - Peierls instability
- $n = 2$: V_2O_3
  - localized electrons
  - electronic correlations
- V_nO_{2n-1}
  - "interpolate" between VO_2 and V_2O_3
  - charge order, orbital order

V_nO_{2n-1}, Ti_nO_{2n-1}

Europhys. Lett. **61**, 361 (2003)
Europhys. Lett. **64**, 682 (2003)
CPL **390**, 151 (2004)
Ann. Phys. **13**, 475 (2004)
J. Phys.: CM **18**, 10955 (2006)

V_2O_3, Ti_2O_3

PRL **86**, 5345 (2001)
PRL **90**, 186403 (2003)
PRB **70**, 205116 (2004)
Europhys. Lett. **70**, 782 (2005)
pss (b) **243**, 2599 (2006)

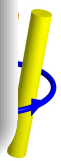

Success Stories

Basics

- DFT (exact, ground state)
- LDA, GGA, . . .

Percus-Levy partition

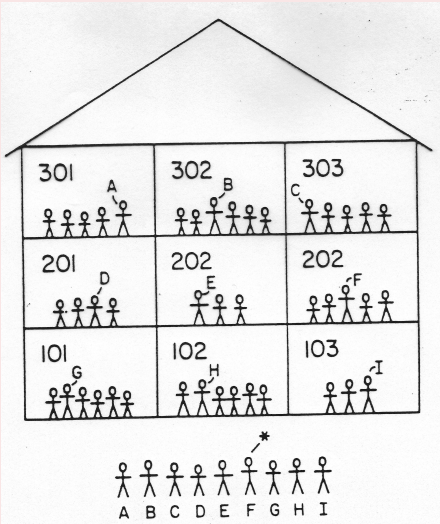

Success Stories

Basics

- DFT (exact, ground state)
- LDA, GGA, . . .

Implementation

- Muffins and beyond
- Full-Potential ASW

Percus-Levy partition

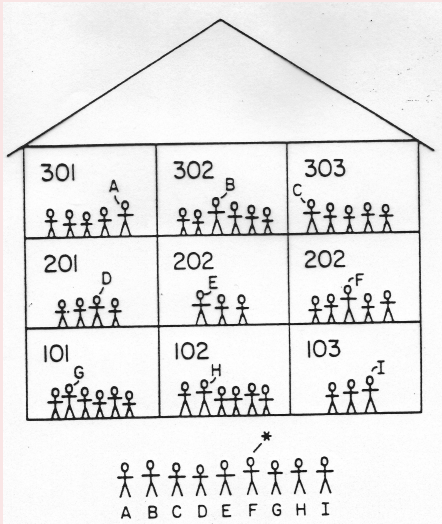

Full-Potential Code

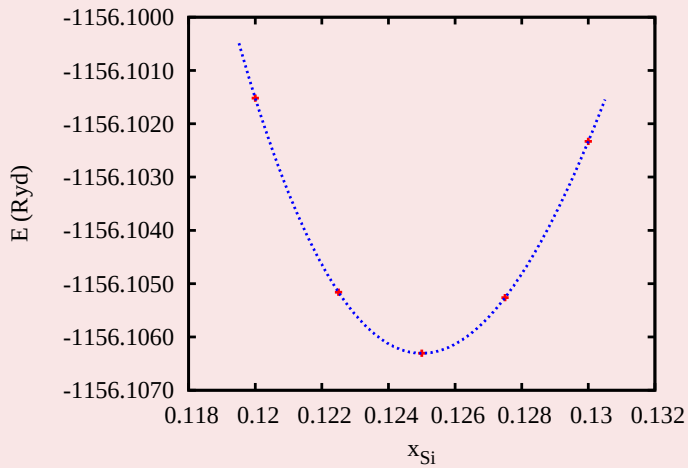

Success Stories

Metal-Insulator Transitions in VO_2

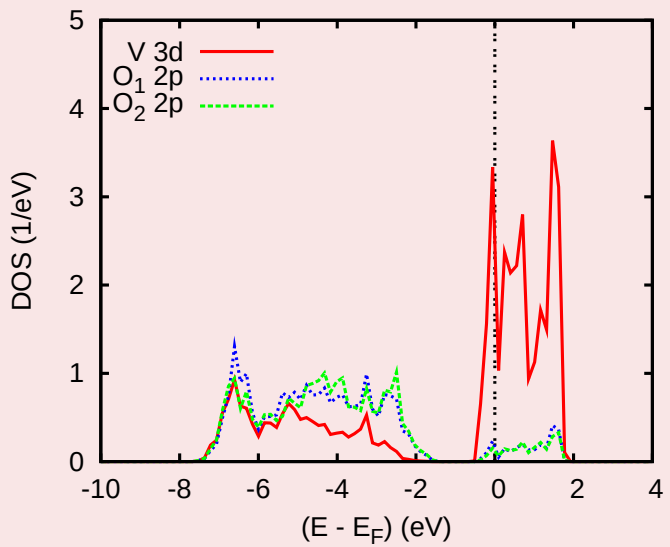

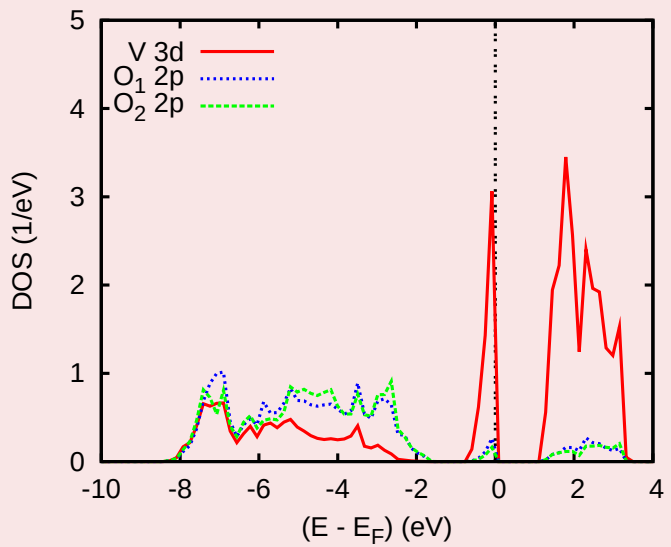

Acknowledgments

Augsburg

U. Eckern, K.-H. Höck,
S. Horn, R. Horny, T. Kopp,
J. Kündel, J. Mannhart,
J. Moosburger-Will

GEFÖRDERT VOM
Bundesministerium
für Bildung
und Forschung

Darmstadt/Jülich

P. C. Schmidt, M. Stephan,
J. Sticht †

Europe/USA

M. Christensen, C. Freeman,
M. Halls, A. Mavromaras, P. Saxe,
E. Wimmer, R. Windiks, W. Wolf

Acknowledgments

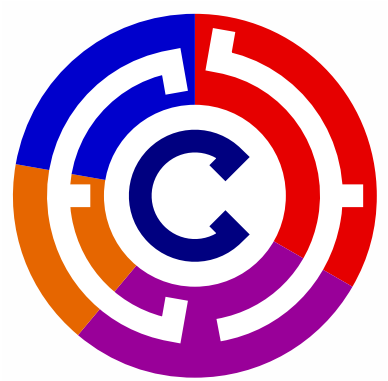

Augsburg

U. Eckern, K.-H. Höck,
S. Horn, R. Horny, T. Kopp,
J. Kündel, J. Mannhart,
J. Moosburger-Will

GEFÖRDERT VOM

Bundesministerium
für Bildung
und Forschung

Darmstadt/Jülich

P. C. Schmidt, M. Stephan,
J. Sticht †

Europe/USA

M. Christensen, C. Freeman,
M. Halls, A. Mavromaras, P. Saxe,
E. Wimmer, R. Windiks, W. Wolf

Bielefeld

Thank You for Your Attention!